Propagating single photons from an open cavity: Description from universal quantization

A. Saharyan [1], B. Rousseaux [1], Z. Kis,[2] S. Stryzhenko [3] and S. Guérin[1,*]

[1]*Laboratoire Interdisciplinaire Carnot de Bourgogne, CNRS UMR 6303, Université de Bourgogne, BP 47870, 21078 Dijon, France*

[2]*Wigner Research Center for Physics, Konkoly-Thege Miklós út 29-33, 1121 Budapest, Hungary*

[3]*Institut für Angewandte Physik, Technische Universität Darmstadt, Hochschulstraße 6, 64289 Darmstadt, Germany*

(Received 8 May 2023; accepted 6 July 2023; published 26 July 2023)

Over the last decades, quantum optics has evolved from high-quality-factor cavities in the early experiments toward new cavity designs involving leaky modes. Despite very reliable models, in the concepts of cavity quantum electrodynamics, photon leakage is most of the time treated phenomenologically. Here, we take a different approach, and starting from first principles, we define an inside-outside representation which is derived from the original true-mode representation, in which one can determine the effective Hamiltonian and Poynting vector. Unlike the phenomenological model, they allow a full description of a leaking single photon produced in the cavity and propagating in free space. This is applied for a laser-driven atom-cavity system. In addition, we propose an atom-cavity nonresonant scheme for single-photon generation, and we rigorously analyze the outgoing single photon in time and frequency domains for different coupling regimes. Finally, we introduce a particular coupling regime ensuring adiabatic elimination for which the pulse shape of the outgoing single photon is tailored using a specifically designed driving field envelope.

DOI: 10.1103/PhysRevResearch.5.033056

I. INTRODUCTION

Single photons are nowadays key elements in quantum technologies, as quantum networking for distributed computation, communication, and metrology [1–7]. Sources producing single photons have been widely developed [8,9]. Their quantization and treatment as wave functions in connection with a corpuscular viewpoint have been debated until recently [10–12]. From a practical point of view, one can, for instance, mention the need for such a description in quantum cryptography [13] over the use of attenuated laser pulses for making the security of quantum key distribution device independent, or for extending quantum communication over very long distances [3,4,14–16]. An envisioned quantum network makes use of single-photon wave packets as carriers of quantum information (encoded, for instance, in the polarization state giving flying qubits) to map the states between distant quantum nodes [3,5,6,17], such as individual atoms in cavity quantum electrodynamics (cavity QED) [18–30], atomic ensembles [31,32], trapped ions [33,34], or spins in quantum dots [35,36]. One key point is to control the node-photon interfacing, i.e., to have control over the produced photon frequency, bandwidth, and temporal shape such that the node can send, receive, store, and release photonic quantum information [33,37–41]. This control is in general achieved by control laser pulses. Recent studies have investigated the control of the shape of the single-photon wave packets in Λ atoms by a resonant stimulated Raman process [42–45] in order, for instance, to improve the impedance matching of the atom-photon interface [25,26]. The possible production of more complex traveling photonic states featuring $N > 1$ photons [46–49] can be envisioned for the transport of complex information. For instance, the delays and relative amplitudes between the pulse-shaped individual photons offer a large variety of encoding, which generalizes the possibility of producing a train of well-separated pulses [50].

Cavity QED, the theory of atoms coupled to single-mode cavities, is nowadays well known [5,51–53]. More recently, transposition of cavity QED to leaky cavities has, however, led to misinterpretations in nanophotonics [54]. These issues are mainly due to a misuse of the models derived for high-quality-factor (high-Q) cavity QED experiments, as opposed to full quantized treatment [55,56]. Indeed, they were derived with a phenomenological system-reservoir approach to describe the cavity leakage, where a flat continuum with a constant coupling is assumed for the reservoir, perturbatively broadening the cavity resonances (see, e.g., comments in Ref. [37]). Derivation from first principles is highly desirable, even for the case of high-Q cavities, since it will provide the community with clearer aspects in the limits of the applicability of these well-known models.

In this paper, we establish such a derivation: Starting from the universal quantization of the true modes in a semi-infinite system composed of a perfectly reflecting boundary and a semitransparent mirror, we determine effective models for a laser-driven atom in a cavity and characterize the resulting propagating photon field. To this aim, we define and connect concepts, namely, photon fluxes, input-output operators,

*sguerin@u-bourgogne.fr

the quantized Poynting vector, the effective master equation, photonic wave packets, and states, to this concrete physical situation [51–53]. We derive an inside-outside representation from first principles, allowing us to characterize the leaking photon in the time domain as well as in the frequency domain. We analyze the validity of different representations, i.e., the true-mode picture, the inside-outside representation, and the pseudomode picture, by comparing the dynamics obtained in each representation. We apply the model for a nonresonant scheme in a three-level atom trapped in a cavity and show that it allows a direct and simple way to design the photonic wave packet on demand. This is obtained for a particular coupling regime, which ensures single-photon production without populating the cavity state. This leads to the production of a single photon with broad bandwidth, which can be of advantage when coupling photon states with materials of distinct resonances.

This paper is organized as follows: In Sec. II, we introduce different representations: true-mode, inside-outside, and pseudomode pictures. From the equivalence of true-mode and inside-outside representations, we write the cavity-reservoir coupling function [57], which is later used to analyze the dynamics of the leaking photon. The explicit form of this coupling function allows one to derive the standard input-output formulation *without applying any a priori approximations* [53,58–60] leading to false mathematical justifications of the Markov approximation (see, e.g., comments in Appendix A). We connect the photon flux, corresponding to the propagation of the photonic state in free space leaking from the cavity to the quantum average of a reservoir photon number operator, in the Heisenberg picture, using the quantized Poynting vector derived from the true-mode representation. The condition of correspondence of this reservoir photon number operator to the standard output photon number operator is derived. We next establish that the photon flux is proportional to the quantum average of the cavity photon number operator in the condition of an initial ground state reservoir. The master equation, which allows one to determine the state of the atom-cavity system, is finally derived. In Sec. III, we apply the derived model to the production of shaped single-photon wave packets, using a nonresonant laser pulse scheme for a three-level atom in a "Λ" configuration inside of a high-Q cavity. We provide a summary in Sec. IV.

II. DERIVATION OF THE MODEL

In this section, we introduce different representations for deriving the dynamics of an atom trapped in an optical cavity and driven by a classical field. In particular, we introduce the inside-outside representation, which assumes separation between the modes of the inside and the outside of the cavity. We analyze the validity of this separation by comparing the dynamics obtained via inside-outside representation to that obtained from the universal quantization of the true, unseparated modes of Maxwell's equations in a one-dimensional semi-infinite space [27,57,61]. We then connect the photon flux [62,63], corresponding to the propagation of the photonic state in free space leaking from the cavity, to the quantum average of a reservoir photon number operator, in the Heisenberg picture, constructed with an integrated reservoir operator. We derive the quantized Poynting vector from the true-mode representation, which we then write in terms of the reservoir operators corresponding to the inside-outside representation. We derive the condition of correspondence of this reservoir photon number operator to the standard output photon number operator derived in the input-output formulation [51]. We next establish that the photon flux is proportional to the quantum average of the cavity photon number operator when the reservoir is initially in the ground state [50]. We finally derive the master equation [51,53,64] by tracing out the reservoir degrees of freedom, which allows one to determine the state of the atom-cavity system, necessary to obtain the quantum averages describing the relevant physical observables.

A. Hamiltonian in the Schrödinger picture

We consider a single Λ atom with ground $|g\rangle$, metastable $|f\rangle$, and excited $|e\rangle$ states trapped in a cavity, which is designed to sustain a field of wavelength λ_c and frequency ω_c. The $|f\rangle \leftrightarrow |e\rangle$ transition, with frequency ω_{ef} and dipole moment d_{fe}, is assumed to be nearly resonant with a cavity mode of area $\mathcal{A}$ and length L, with the detuning $\Delta_c = \omega_{ef} - \omega_c$; the $|g\rangle \leftrightarrow |e\rangle$ transition, with frequency ω_{eg} and dipole moment d_{ge}, is assumed to be independently driven by a classical laser field $\mathcal{E}(t)\cos(\omega_0 t + \varphi)$, corresponding to the time-dependent Rabi frequency $\Omega(t) = -\mathcal{E}(t)d_{ge}/2\hbar$, with a detuning $\Delta = \omega_{eg} - \omega_0$. In this paper, we assume the mirrors of the cavity to be large enough that the spontaneous emission of the atom in modes propagating in directions perpendicular to the optical axis can be neglected. Thus we consider the cavity to be a one-dimensional Fabry-Pérot resonator.

1. True-mode representation

The universal quantization procedure [27,57,61,65,66] is a derivation from first principles, which allows the treatment of the cavity as part of the environment and the derivation of true (exact) modes for such a closed system (see Fig. 1). Here we consider the same physical situation as the one in Ref. [57], where the cavity is delimited by a perfect mirror on the left and a semitransparent mirror on the right, the latter being made of a single layer of a dielectric material. The length of the dielectric layer is considered to be negligible with respect to the cavity length. By introducing an atom in such a cavity, we can write the Hamiltonian for the full system $\mathcal{A} \oplus \mathcal{E}$ in a rotating frame defined by the unitary operator $U_{\rm RW} = \exp(-i\omega_0 t)\sigma_g + \sigma_e + \sigma_f$:

$$\tilde{H}(t) = H_A(t) + H_{\rm int} + H_E, \tag{1a}$$

$$H_A(t) = \hbar(\Delta - \Delta_c - \omega_c)\sigma_f + \hbar\Delta\sigma_e + \hbar\Omega(\sigma_{ge} + \sigma_{eg}), \tag{1b}$$

$$H_E = \int_0^{+\infty} d\omega\, \hbar\omega a_\omega^\dagger a_\omega, \tag{1c}$$

$$H_{\rm int} = i\hbar \int_0^{+\infty} d\omega\, (\eta(\omega)a_\omega\sigma^\dagger - \eta^*(\omega)a_\omega^\dagger\sigma), \tag{1d}$$

where $H_A \equiv H_A(t)$ denotes the atomic Hamiltonian in the rotating wave approximation (RWA). Here, we have introduced the atomic operators $\sigma_{k\ell} \equiv |k\rangle\langle\ell|$, $\sigma_k \equiv \sigma_{kk}$, and $\sigma \equiv \sigma_{fe}$. H_E describes the environment with the cavity as part of it. Operators a_ω, $a_\omega^\dagger$ are the annihilation and creation operators for the

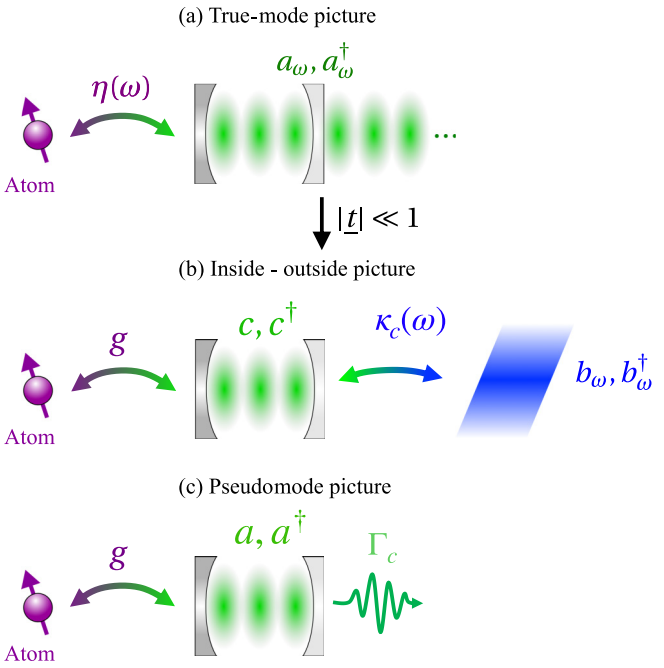

FIG. 1. (a) True-mode picture corresponding to the modes obtained from universal quantization, where the cavity is treated as part of the environment. In such a representation, the atom is coupled to the universal modes a_ω with a frequency-dependent coupling strength $\eta(\omega)$. (b) For cavities with sufficiently small transmission it is possible to approximately separate modes into cavity (inside) and reservoir (outside) modes, with an effective frequency-dependent coupling $\kappa_c(\omega)$. In this picture, the atom couples mainly to the cavity mode c, to which it is resonant (or near resonant), with coupling strength g. (c) Unlike the two other representations, in the pseudomode picture, the reservoir is eliminated and accounted for via the cavity decay rate Γ_c, in a non-Hermitian description.

true modes, satisfying the commutation relation

$$[a_\omega, a_{\omega'}^\dagger] = \delta(\omega - \omega'). \tag{2}$$

H_{int} represents the interaction between the atom and the structured environment, with the coupling factor

$$\eta(\omega) = i\sqrt{\frac{\omega}{\hbar\epsilon_0\pi c\mathcal{A}}}d_{fe}\, e^{i\frac{\omega}{c}L}\sin\left(\frac{\omega}{c}(x_A + L)\right)T(\omega) \tag{3a}$$

$$\approx i\sqrt{\frac{\omega}{\hbar\epsilon_0 L\mathcal{A}}}d_{fe}\, e^{i\frac{\omega}{c}L}\sin\left(\frac{\omega}{c}(x_A + L)\right) \times\sqrt{\frac{\Gamma_c}{2\pi}}\frac{1}{\omega - \omega_c + i\frac{\Gamma_c}{2}}, \tag{3b}$$

where $T(\omega)$ is the single-layer cavity response function and x_A is the position of the atom. For a cavity with sufficiently high reflectivity the response function can be represented as a sum of mode-selective Lorentzian functions, whose width Γ_c (decay rate of the cavity) is much smaller than the spacing $\Delta_\omega = \pi c/L$ between the neighboring resonances (high-finesse cavity) [27,57,61] (see details in Appendix B). For a single-layer partially transparent cavity mirror, high reflectivity can be achieved by assuming a fictitiously large refractive index of the dielectric material, while for more realistic models high reflectivity implies a cavity mirror made of a large number

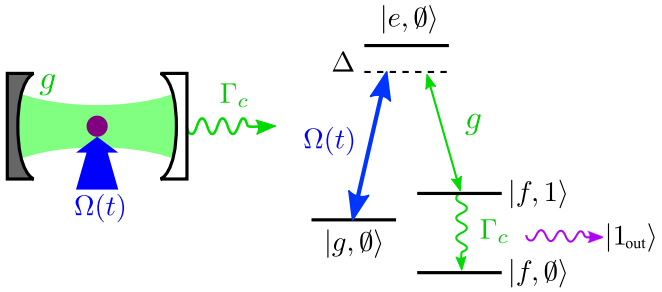

FIG. 2. Atom-field interaction in the cavity. Left panel: A single Λ atom is driven by an external classical laser field of Rabi frequency Ω and a quantized cavity field with coupling strength g. Right panel: The fields are in two-photon resonance ($\Delta = \Delta_c$), and the one-photon detuning is Δ. Initially, the atom is in the ground state $|g\rangle$. In the course of the excitation process, one photon is taken from the laser field and transferred to the cavity, which eventually leaks out of the cavity through a semitransparent mirror characterized by the decay rate Γ_c.

of dielectric layers [27]. In the literature, these assumptions usually correspond to the high-Q cavity limit. However, as we show below, the high-Q assumption by itself is not sufficient, by definition. Instead, we should require a high-finesse cavity, which satisfies all the conditions necessary to perform the above approximations.

In Eq. (3b), we assume that the atom couples to a single mode (ω_c), reducing the sum of Lorentzians into a single one. The Hamiltonian (1) with the coupling (3) describes a true-mode representation, i.e., with continuous frequencies, but with a structured reservoir [67]. In the following we break these true modes into inside and outside modes, which describe the cavity and the reservoir separately.

2. *Mode separation into inside and outside modes*

We now consider an approximately equivalent model to the one obtained previously via splitting the modes a_ω into two parts: cavity modes c (inside) and the continuum of reservoir modes b_ω (outside) [Fig. 1(b)]. The derivation is formally shown in Ref. [57], exhibiting an error of order $O(|\underline{t}|^2)$, where $\underline{t}$ is the transmission rate of the (single layer) mirror. This representation can be interpreted as replacing the semitransparent mirror with a perfect one, forming a perfect cavity ($\mathcal{C}$), which is coupled to the reservoir ($\mathcal{R}$) [57] (see Fig. 2 for the coupling scheme of the atom with the cavity). We refer to it as the inside-outside representation. The RWA Hamiltonian of the full system $\mathcal{A} \oplus \mathcal{C} \oplus \mathcal{R}$ reads, in the Schrödinger picture:

$$H(t) = H_A(t) + H_{AC} + H_C + H_{RC} + H_R, \tag{4a}$$

$$H_C = \hbar\omega_c c^\dagger c, \tag{4b}$$

$$H_{AC} = \hbar g(c^\dagger\sigma + \sigma^\dagger c), \tag{4c}$$

$$H_R = \int_0^{+\infty} d\omega\, \hbar\omega\, b_\omega^\dagger b_\omega, \tag{4d}$$

$$H_{RC} = i\hbar\int_0^{+\infty} d\omega\, (\kappa_c(\omega)b_\omega^\dagger c - \kappa_c^*(\omega)c^\dagger b_\omega), \tag{4e}$$

with the atom-cavity coupling factor $g = -d_{fe}\sqrt{\omega_c/\hbar\epsilon_0 L\mathcal{A}}$ (one-photon Rabi frequency), assuming the atom is localized

at the field maximum. The coupling factor $\eta(\omega)$ for the true-mode picture [Eq. (3b)] can then be approximated as [27]

$$\eta(\omega) \approx \hat{\eta}(\omega) = -ig\sqrt{\frac{\Gamma_c}{2\pi}}\frac{1}{\omega - \omega_c + i\frac{\Gamma_c}{2}}. \tag{5}$$

This form allows the direct derivation of the pseudomode representation described below [see Eq. (8)].

In Eq. (4), $H_A(t)$ is the same as Eq. (1b), H_C is the free-cavity Hamiltonian, H_{AC} describes the coupling between the atom and the cavity, H_R is the free-reservoir Hamiltonian, and H_{RC} describes the coupling between the empty cavity and the free reservoir. The reservoir annihilation and creation operators b_ω, $b_\omega^\dagger$ satisfy the commutation relation

$$[b_\omega, b_{\omega'}^\dagger] = \delta(\omega - \omega'). \tag{6}$$

The cavity-reservoir coupling function $\kappa_c(\omega)$ can be evaluated in the limit of small transmission and near resonance as [57]

$$\kappa_c(\omega) = -i\sqrt{\frac{\Gamma_c}{2\pi}}e^{-i\frac{\omega}{c}L}\mathrm{sinc}\left((\omega - \omega_c)\frac{L}{c}\right). \tag{7}$$

To derive this function, as demonstrated in Ref. [57], one should first derive the modes corresponding to Maxwell's equations in a one-dimensional semi-infinite space incorporating a cavity made of a partially transparent single-layer mirror with negligible mirror thickness. Then, one can consider a model where the actual cavity is replaced by a perfect one which is then coupled to the semi-infinite reservoir delimited by the perfect cavity. By equating the inside modes of the partially transparent cavity obtained from Maxwell's equations to the discrete perfect cavity modes, and doing the same for the corresponding modes describing the outside, the expression in (7) can be obtained for sufficiently small transmission. We highlight that in this derivation there is no emitter initially considered in the system, and the coupling function $\kappa_c(\omega)$ describes the coupling of the empty cavity to the environment.

One can notice that the derived inside-outside representation does not feature the constant cavity-reservoir coupling that is generally assumed in the standard derivation under certain conditions [51]. The standard approach, albeit leading to physically accurate results, can lead to mathematical inconsistencies (see Appendix A). Here, however, the cavity-reservoir coupling has a specific form (7), which is obtained under mathematically explicitly defined conditions [57] and can be treated straightforwardly.

3. Pseudomode representation

We can define a pseudomode representation via [27]

$$\hat{H}(t) = H_A(t) + \hat{H}_{AC} + \hat{H}_C, \tag{8a}$$

$$\hat{H}_{AC} = \hbar g(a^\dagger\sigma + \sigma^\dagger a), \tag{8b}$$

$$\hat{H}_C = \hbar\left(\Delta - \Delta_c - i\frac{\Gamma_c}{2}\right)a^\dagger a, \tag{8c}$$

where, for a single mode,

$$a^\dagger|\emptyset\rangle = |1\rangle. \tag{9}$$

This representation is derived directly from the true-mode picture with the approximate coupling (5). In general, the cavity mode c in (4) and a in (8) are different. c is the perfect cavity mode, while a is defined as [27]

$$a = \frac{1}{g}\int d\omega\, \hat{\eta}(\omega)\hat{a}_\omega, \tag{10}$$

where $\hat{a}_\omega$ is the annihilation operator of the mode defined for the approximate coupling $\hat{\eta}(\omega)$.

We highlight that Hamiltonian (8) is for the open system $\mathcal{A} \oplus \mathcal{C}$, where the reservoir is eliminated, while Hamiltonians (1) and (4) both describe closed systems. Here, the annihilation operators a and c represent physically the same approximate modes but are derived differently. In the following we analyze these different representations by comparing the dynamics obtained via each Hamiltonian.

4. Comparison and validity of the different representations

We numerically analyze the validity of different representations described in Fig. 1. We consider a single atom trapped in the cavity and assume an initial condition with zero photons. To differentiate the parameters of different representations, we denote the quantities corresponding to the true-mode picture and the pseudomode picture with a tilde and a hat, respectively. We commence by deriving the dynamics corresponding to the true-mode representation. Here, one can denote the basis as $|i\rangle|\alpha\rangle \equiv |i, \alpha\rangle$, with i labeling the atomic states and α describing the state of the continuum. The state in this basis can then be given by the following wave function:

$$|\tilde{\psi}\rangle = \tilde{c}_{g,0}(t)|g, \emptyset\rangle + \tilde{c}_{e,0}(t)|e, \emptyset\rangle + \int_0^{+\infty} d\omega\, \tilde{c}_{f,1}(\omega, t)|f, \mathbf{1}_\omega\rangle, \tag{11}$$

with

$$a_\omega^\dagger|\emptyset\rangle = |\mathbf{1}_\omega\rangle, \tag{12a}$$

$$a_\omega|\mathbf{1}_{\omega'}\rangle = \delta(\omega - \omega')|\emptyset\rangle. \tag{12b}$$

Using Hamiltonian (1) in the time-dependent Schrödinger equation with state (11), we obtain the following dynamical equations:

$$i\dot{\tilde{c}}_{g,0}(t) = \Omega\,\tilde{c}_{e,0}(t), \tag{13a}$$

$$i\dot{\tilde{c}}_{e,0}(t) = \Delta\,\tilde{c}_{e,0}(t) + \Omega\,\tilde{c}_{g,0}(t) + i\int_0^{+\infty} d\omega\, \eta(\omega)\,\tilde{c}_{f,1}(\omega, t), \tag{13b}$$

$$i\dot{\tilde{c}}_{f,1}(\omega, t) = (\Delta - \Delta_c + \omega - \omega_c)\tilde{c}_{f,1}(\omega, t) - i\eta^*(\omega)\tilde{c}_{e,0}(t), \tag{13c}$$

where $\eta(\omega)$ is the actual coupling function (3a). If we take into account the approximation in (5), similar equations to (13) can be obtained for a state given by

$$|\hat{\psi}\rangle = \hat{c}_{g,0}(t)|g, \emptyset\rangle + \hat{c}_{e,0}(t)|e, \emptyset\rangle + \int_0^{+\infty} d\omega\, \hat{c}_{f,1}(\omega, t)|f, 1_\omega\rangle, \tag{14}$$

with $|1_\omega\rangle = \hat{a}_\omega^\dagger|\emptyset\rangle$. Here, we can define the photon state of the cavity as [27]

$$|1\rangle = \frac{1}{g}\int_0^{+\infty} d\omega\, \hat{\eta}^*(\omega)\hat{a}_\omega^\dagger|\emptyset\rangle, \tag{15}$$

which follows from the definition (10). Consequently, by using Hamiltonian (8) we get the dynamics corresponding to the pseudomode representation, on a reduced basis $\{|g,\emptyset\rangle, |e,\emptyset\rangle, |f,1\rangle\}$, for the state given by

$$|\psi_{\text{eff}}\rangle = \hat{c}_{g,0}(t)|g,\emptyset\rangle + \hat{c}_{e,0}(t)|e,\emptyset\rangle + \hat{c}_{f,1}(t)|f,1\rangle,$$

$$i\dot{\hat{c}}_{g,0}(t) = \Omega\,\hat{c}_{e,0}(t), \tag{16a}$$
$$i\dot{\hat{c}}_{e,0}(t) = \Delta\,\hat{c}_{e,0}(t) + \Omega\,\hat{c}_{g,0}(t) + g\,\hat{c}_{f,1}(t), \tag{16b}$$
$$i\dot{\hat{c}}_{f,1}(t) = \left(\Delta - \Delta_c - i\frac{\Gamma_c}{2}\right)\hat{c}_{f,1}(t) + g\,\hat{c}_{e,0}(t). \tag{16c}$$

Unlike the case of the true-mode picture, in the inside-outside representation there is a separation of the photon state into inside and outside ones. Thus the basis splits into the following states: $\{|g,\emptyset\rangle, |e,\emptyset\rangle, |f,1_{\text{in}},\emptyset_{\text{out}}\rangle, |f,\emptyset_{\text{in}},1_{\omega,\text{out}}\rangle\}$, where the indices "in" and "out" indicate the photon state inside and outside the cavity, respectively, and

$$c^\dagger|\emptyset\rangle = |1_{\text{in}}\rangle, \tag{17a}$$
$$c|1_{\text{in}}\rangle = |\emptyset\rangle, \tag{17b}$$
$$b^\dagger_\omega|\emptyset\rangle = |1_{\omega,\text{out}}\rangle, \tag{17c}$$
$$b_\omega|1_{\omega',\text{out}}\rangle = \delta(\omega-\omega')|\emptyset\rangle. \tag{17d}$$

The dynamical equations corresponding to the Hamiltonian (4) with the state

$$|\psi\rangle = c_{g,0}(t)|g,\emptyset\rangle + c_{e,0}(t)|e,\emptyset\rangle + c_{f,1,0}(t)|f,1_{\text{in}},\emptyset_{\text{out}}\rangle + \int_0^{+\infty} d\omega\, c_{f,0,1}(\omega,t)|f,\emptyset_{\text{in}},1_{\omega,\text{out}}\rangle \tag{18}$$

become

$$i\dot{c}_{g,0}(t) = \Omega\,c_{e,0}(t), \tag{19a}$$
$$i\dot{c}_{e,0}(t) = \Delta\,c_{e,0}(t) + \Omega\,c_{g,0}(t) + g\,c_{f,1,0}(t), \tag{19b}$$
$$i\dot{c}_{f,1,0}(t) = (\Delta-\Delta_c)c_{f,1,0} + g\,c_{e,0}(t) - i\int_0^{+\infty} d\omega\,\kappa_c^*(\omega)\,c_{f,0,1}(\omega,t), \tag{19c}$$
$$i\dot{c}_{f,0,1}(\omega,t) = (\Delta-\Delta_c+\omega-\omega_c)c_{f,0,1}(\omega,t) + i\kappa_c(\omega)\,c_{f,1,0}(t). \tag{19d}$$

In order to examine the validity limits of the approximate models derived above, we compare the dynamics via solving Eqs. (13), (16), and (19) [see details of the integration of Eqs. (13) and (19) in Appendix C]. For this analysis, the way the atom is driven to its excited state is irrelevant. Thus we assume that the atom is initially in the excited state $|e\rangle$ and there is no laser field applied, i.e., $\Omega = 0$. We analyze a regime where there are no Rabi oscillations between the atom and the produced photon, i.e., the leakage from the cavity is stronger than the atom-cavity coupling: $\Gamma_c > g$. Both the effective Hamiltonian and the inside-outside representation are derived under the assumption of having a high-Q cavity, i.e., $\Gamma_c \ll \omega_c$. In Fig. 3, we present the results obtained via different representations for a cavity with a fixed quality factor: $\omega_c/\Gamma_c \approx 1200$. This factor is obtained either by fixing the mirror refractive index and changing the length of the cavity or vice versa. In Fig. 3(a), the cavity length is such that it sustains half a wavelength of cavity resonance wavelength λ_c: $L = L_0 = \lambda_c/2$. Therefore there is only a single mode that the atom can couple to, making the cavity finesse the same as the quality factor: $\Delta_\omega/\Gamma_c \approx 1200$. As we can see from the figure, both for detuned and nondetuned cases, the photons obtained with pseudomode and inside-outside representations match the true-mode representation obtained from Eq. (13), with the coupling (3a) [68]. Furthermore, in Fig. 3(b), we consider a cavity of longer length and a mirror of lower refractive index. To have the same atom-cavity coupling rate, we change the value of the dipole moment of the atom. While having the same quality factor, here we get a cavity finesse $\Delta_\omega/\Gamma_c \approx 7$. This low finesse makes the transition from Eq. (3a) to Eq. (3b) less accurate, i.e., the Lorentzians corresponding to each mode are not separated well enough to consider $\sqrt{\sum f_m} \approx \sum \sqrt{f_m}$. We emphasize that the approximation (3b) is used in the derivation of the pseudomode picture as well as the inside-outside representation. Hence it leads to a mismatch between the approximate and the actual representations. Equivalently, as shown in Ref. [27], in order for the pseudomode derivation to work, the following condition should hold: $(\frac{\Gamma_c}{c}(x_A + L))^2 \ll 1$. Evidently, when we increase the cavity length while keeping Γ_c the same, this condition is not well satisfied, breaking the validity of this representation. On the other hand, as mentioned before, the inside-outside representation is derived for the cavities with low transmission rate, given by $|\underline{t}|^2 = 1 - e^{-2L\Gamma_c/c}$ (see Appendix B). For this long-cavity scenario, similar to the previous argument, this term fails to satisfy the condition $|\underline{t}|^2 \ll 1$ ($|\underline{t}|^2 \approx 0.58$), which leads to the mismatch between the inside-outside and the true-mode representations. Finally, we can notice that even in the case of $\Delta_c = 0$, the photon obtained from the actual model is slightly shifted from the resonance frequency ω_c. This is because in the actual model where we use the response function $T(\omega)$, apart from the fundamental mode ω_c, there are other modes, which, combined with the low finesse of the cavity, affect the produced photon.

In Figs. 3(c) and 3(d), we study the corresponding photon shape in the time domain. Here we compare the cavity photon state obtained from the pseudomode $[\hat{c}_{f,1}(t)]$ and the inside-outside representations $[c_{f,1,0}(t)]$. As we can see from Eq. (16), the photon state $\hat{c}_{f,1}(t)$ depends only on the parameters Γ_c and g, and these parameters are fixed; hence $\hat{P}_{f,1}$ is the same for both high-finesse [Fig. 3(c)] and low-finesse [Figs. 3(d)] scenarios. On the other hand, in the inside-outside representation, the coupling $\kappa_c(\omega)$ explicitly depends on the cavity length, leading to different curves for the state $P_{f,1}$. This, combined with the arguments introduced in the analysis of Figs. 3(a) and 3(b), leads to the differences between the photons obtained via pseudomode and inside-outside representations.

In the following, we derive the well-known master equation starting from the inside-outside representation. We use

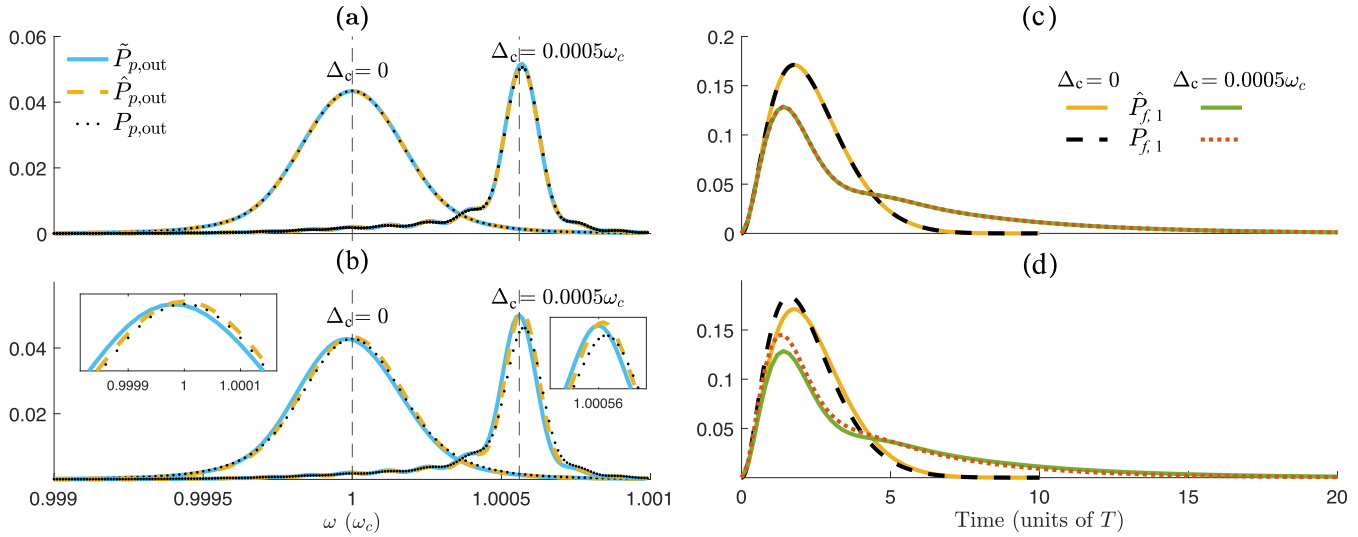

FIG. 3. Comparison of the single-photon shape obtained via true-mode, inside-outside, and pseudomode pictures. (a) and (b) Spectral shapes of the outgoing photon with $(|g|, \Gamma_c, \omega_c) \times T = (0.6, 2, 2416)$, where $\omega_c = m\frac{\pi c}{L}$, m being the number of antinodes inside the cavity. Each curve corresponds to a different representation: $\tilde{P}_{p,\text{out}} = |\tilde{\mathbf{c}}_{f,1}(\omega, t_\text{f})|^2$ (true-mode picture), $\hat{P}_{p,\text{out}} = |\hat{\mathbf{c}}_{f,1}(\omega, t_\text{f})|^2$ (pseudomode picture), and $P_{p,\text{out}} = |\mathbf{c}_{f,0,1}(\omega, t_\text{f})|^2$ (inside-outside picture; see the definition of the dimensionless parameters $\mathbf{c}_i$ in Appendix C), where t_f is the final time when the photon is in its steady state. In (a), $t_\text{f}/T = 10$, $\Gamma_c = 2/T$ is obtained for a cavity with a length $L = L_0$ and a fictitious refractive index $n = 27.735$, leading to the reflectivity $R = |\underline{r}|^2 = e^{-2L\Gamma_c/c} \approx 0.995$ (with $\frac{L_0}{cT} = 0.0013$), where L_0 is the length for which the cavity sustains a single fundamental mode, i.e., $m = 1$. In (b), $t_\text{f}/T = 20$, $L = 165L_0$, and $n = 2.1756$, leading to the same $\Gamma_c = 2/T$, for the $m = 165$th mode, with the reflectivity $R \approx 0.42$. (c) and (d) Time profiles of the outgoing photon, obtained via the same parameters introduced in (a) and (b), respectively. $\hat{P}_{f,1} = |\hat{c}_{f,1}(t)|^2$, $P_{f,1} = |c_{f,1,0}(t)|^2$ are the photon states derived from the pseudomode and inside-outside representations, respectively.

a method different from the standard derivation obtained by phenomenological use of the pseudomode Hamiltonian.

B. Heisenberg-Langevin equations, Poynting vector, and photon fluxes

We wish to derive the effective dynamics of the atom-cavity system $\mathcal{S} = \mathcal{A} \oplus \mathcal{C}$, coupled to the reservoir, from first principles. Our aim is to control the production of an outgoing photon leaking from the cavity by driving specifically the atom in the cavity by the external field. We will use the convenient inside-outside representation as it will allow a clear identification and characterization of the leaking photon propagating in free space. Here, we study the case presented in Fig. 2, where the atom is initially in the ground state, and we consider the two-photon resonance condition: $\Delta = \Delta_c$, leading to $\omega_{gf} = \omega_c - \omega_0$. We use the Poynting vector that we derive from the true-mode representation and define in the Heisenberg picture. We highlight that one could use the Poynting vector derived in Ref. [62] and generalize it to the situation with the presence of a cavity; however, as we show below, the Poynting vector that we derive from first principles is different from this one. We then derive the effective model in two steps: We first define an outgoing flux of photons which is connected to the quantum average of the Heisenberg evolution of the cavity operator $c^\dagger c$. Next, we derive a master equation of the system $\mathcal{S}$ by eliminating the reservoir degrees of freedom, which will allow the calculation of the quantum averages.

1. *Equations of motion for the operators*

First, we derive the equations of motion in the Heisenberg picture for the reservoir operator $b_\omega(t) \equiv U^\dagger(t, t_0) b_\omega U(t, t_0)$ with $U(t, t_0)$ being the propagator of the total Hamiltonian $H(t)$, whose Heisenberg picture reads $H^{(H)}(t) = U^\dagger(t, t_0) H(t) U(t, t_0)$. From $\dot{\mathcal{O}} = -\frac{i}{\hbar}[\mathcal{O}(t), H^{(H)}(t)]$ for an operator $\mathcal{O}$, assumed to be time independent in the Schrödinger picture and written as $\mathcal{O}^{(H)}(t) \equiv \mathcal{O}(t) = U^\dagger(t, t_0)\mathcal{O}U(t, t_0)$ in the Heisenberg picture, we write the Heisenberg-Langevin equations:

$$\dot{b}_\omega(t) = -i\omega b_\omega(t) + \kappa_c(\omega) c(t), \tag{20a}$$

$$\dot{c}(t) = -i\omega_c c(t) - \int_0^{+\infty} d\omega\, \kappa_c^*(\omega) b_\omega(t) - ig\sigma(t). \tag{20b}$$

In the following, we omit the "(H)" superscript for the Heisenberg picture Hamiltonian $H^{(H)}(t) \equiv H(t)$. The energy carried by the photons leaking from the cavity can be characterized by the Poynting vector operator in the Heisenberg picture. We derive the Poynting vector, using the electromagnetic fields outside the cavity in the true-mode representation [27,57,61] (see details of the derivation in Appendix D):

$$S(x, t) = \frac{\hbar}{2\pi\mathcal{A}} \int_0^\infty d\omega d\omega' \sqrt{\omega\omega'} R_\omega R_{\omega'}^* e^{i(\omega-\omega')\frac{x}{c}} a_{\omega'}^\dagger(t) a_\omega(t), \tag{21}$$

where the expression of R_ω is given in Appendix D. Via moving from the true-mode representation to the inside-outside representation, we get the following Poynting vector

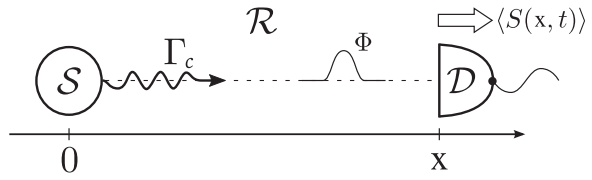

FIG. 4. Sketch of the photodetection: The source system $\mathcal{S}$ emits a photon with decay rate Γ_c at position 0, towards a detector $\mathcal{D}$ at a position x through the reservoir $\mathcal{R}$. The photon flux Φ is measured using the data on the averaged quantized Poynting vector $\langle S(x,t)\rangle$.

(Appendix D):

$$S(x,t) = \frac{\hbar\omega_c}{\mathcal{A}} b^\dagger(x,t) b(x,t), \tag{22}$$

where we have introduced the integrated reservoir operator

$$b(x,t) := \frac{1}{\sqrt{\Gamma_c}} \int_0^\infty d\omega \kappa_c^*(\omega) e^{i\frac{\omega}{c}x} b_\omega(t). \tag{23}$$

Taking this into account, we can define a single-photon state propagating from the cavity via leakage Γ_c ($\kappa_c(\omega)$) and defined for $x > 0$:

$$|1_{\text{out}}(x,t)\rangle = b^\dagger(x>0,t)|\emptyset\rangle, \tag{24}$$

where we have assumed a propagation with increasing x and the cavity emitter at position $x = 0$ (see Fig. 4). We emphasize that the time dependence arises only from the Heisenberg picture of the reservoir operator b_ω.

2. Integrated reservoir operators: Input-output relation

In Eq. (23) we have defined the integrated reservoir operator, which we calculate by integrating (20a) from an initial time t_0 to t,

$$b(x,t) := \frac{1}{\sqrt{\Gamma_c}} \int_0^{+\infty} d\omega\, \kappa_c^*(\omega) b_\omega(t) e^{i\omega\frac{x}{c}} \tag{25a}$$

$$= b_{\text{in}}\left(t - \frac{x}{c}\right) + \int_{t_0}^t dt' \int_0^{+\infty} d\omega \frac{|\kappa_c(\omega)|^2}{\sqrt{\Gamma_c}} c(t') \times e^{-i\omega(t-t')} e^{i\omega\frac{x}{c}}, \tag{25b}$$

with the *input* operator defined similarly:

$$b_{\text{in}}\left(t - \frac{x}{c}\right) := \frac{1}{\sqrt{\Gamma_c}} \int_0^{+\infty} d\omega\, \kappa_c^*(\omega) b_\omega(t_0) e^{-i\omega(t-t_0-\frac{x}{c})}. \tag{26}$$

One can notice that the definition (25a) is different from the standard definition, where $b(x,t)$ is defined via a Fourier transform of b_ω [51,69,70] and a flat continuum (see Appendix A). Instead, here we have the natural introduction of the function $\kappa_c(\omega)$ in the definition, and its explicit form allows one to straightforwardly derive the equation for the output operator.

In order to evaluate the integral over the frequency in (25b), we use the expression (7). This gives for the integrated reservoir operator (see details in Appendix E):

$$b(x,t) = b_{\text{in}}\left(t - \frac{x}{c}\right) + \sqrt{\Gamma_c} c\left(t - \frac{x}{c}\right), \tag{27}$$

where we have assumed $t \gg \frac{2L}{c}$, $t > t_0 + \frac{x}{c} + \frac{2L}{c}$. We further neglect the cavity length, assuming that the traveling distance of interest is much larger than the cavity length. Also, considering that the dynamics evolves over a much longer period of time than the round trip time $\frac{2L}{c}$ of the produced photon (coarse-grained approximation), we get $t \gg 0, t > t_0 + \frac{x}{c}$, and $x > 0$. We define the *output* operator

$$b_{\text{out}}(t - x/c) := b(x > 0, t); \tag{28}$$

hence

$$b_{\text{out}}\left(t - \frac{x}{c}\right) = b_{\text{in}}\left(t - \frac{x}{c}\right) + \sqrt{\Gamma_c}\, c\left(t - \frac{x}{c}\right), \tag{29}$$

which is recognized as the input-output relation [51]. We highlight that the input-output relation here is a consequence of the concrete form of $\kappa_c(\omega)$ [Eq. (7)], which justifies thus the Markov approximation. This formulation allows direct and transparent interpretation of the b_{out} operator through the Poynting vector as shown below [see Eq. (33)].

At the cavity position, $x = 0$, we obtain the integrated reservoir operator (see Appendix E):

$$b_0(t) \equiv b(x=0,t) = b_{\text{in}}(t) + \frac{\sqrt{\Gamma_c}}{2} c(t). \tag{30}$$

This expression (30) is used in the next section to derive the master equation in the cavity.

We can also simplify the Heisenberg-Langevin equation for $c(t)$ as

$$\dot{c}(t) = -\left(i\omega_c + \frac{\Gamma_c}{2}\right) c(t) - \sqrt{\Gamma_c} b_{\text{in}}(t) - ig\sigma(t). \tag{31}$$

3. Photon flux

Using the results obtained in the previous section, we can write the Poynting vector (22) in the inside-outside representation as follows:

$$S(x>0,t) = \frac{\hbar\omega_c}{\mathcal{A}} b^\dagger\left(t - \frac{x}{c}\right) b\left(t - \frac{x}{c}\right). \tag{32}$$

For a given state (or density matrix), the amount of energy going through the field mode area $\mathcal{A}$, during the time dt, is the quantum average of the flux of the Poynting vector through this area: $\mathcal{A}\langle S(x,t)\rangle dt = \hbar\omega_c \langle b^\dagger(x,t) b(x,t)\rangle dt$. Normalizing by $\hbar\omega_c$, we get the averaged number of photons $dn(x,t) \equiv \langle b^\dagger(x,t) b(x,t)\rangle dt$ going through the mode area during dt, defining the photon flux (written here for $x > 0$):

$$\Phi(x,t) := \frac{dn(x,t)}{dt} = \left\langle b^\dagger\left(t - \frac{x}{c}\right) b\left(t - \frac{x}{c}\right)\right\rangle. \tag{33}$$

Recalling that $b(t - x/c)$ is the output operator (28), we emphasize that this relation gives the connection between the photon flux and this output operator.

If we choose the state of the reservoir to be initially a vacuum state, $\rho(t_0) = \rho_S(t_0) \otimes |\emptyset\rangle\langle\emptyset|$, the average of the terms involving b_{in}, $b_{\text{in}}^\dagger$ in the expression of the flux is nullified. This gives the expression of the outgoing photon flux through the semitransparent mirror for $t > t_0 + \frac{x}{c}, x > 0$:

$$\Phi(x,t) = \Gamma_c \left\langle c^\dagger\left(t - \frac{x}{c}\right) c\left(t - \frac{x}{c}\right)\right\rangle. \tag{34}$$

This key result shows that one can determine the flux from the quantum average of the dynamics of the cavity photon number in the Heisenberg picture [50].

In the following section, we derive the effective master equation reduced to the system $\mathcal{S}$ which is used to calculate the quantum average of (33) in order to derive the flux.

C. The master equation for the system dynamics

The system dynamics from the above inside-outside representation can be characterized by a master equation which is shown to be of Lindblad form. We follow the derivation of Refs. [51,53,71,72]. We need first to derive the Heisenberg equation of motion of the operators $X_S(t) = U^\dagger(t,t_0)X_S U(t,t_0)$ of the system in the Heisenberg picture.

The dynamics of $X_S(t)$ is determined from the Heisenberg-Langevin equation (see details of the following calculation in Appendix F):

$$\frac{d}{dt}X_S(t) = -\frac{i}{\hbar}\big[X_S(t), H_S^{(H)}(t)\big] + \mathcal{D}^\dagger_{\text{in},t}(X_S(t)) + \Gamma_c\left(c^\dagger(t)X_S(t)c(t) - \frac{1}{2}\{c^\dagger(t)c(t), X_S(t)\}\right), \tag{35}$$

where $\{A,B\} = AB + BA$ denotes the anticommutation relation, $\mathcal{D}^\dagger_{\text{in},t}(\cdot)$ is a time-dependent dissipator part involving $b_{\text{in}}(t)$, acting on $X_S(t)$, and $H_S^{(H)}(t) = U^\dagger(t,t_0)H_S(t)U(t,t_0)$, with H_S being the system Hamiltonian

$$H_S(t) = H_A + H_{AC} + H_C. \tag{36}$$

In Eq. (35) we have used the integrated reservoir operator (30) at the position $x = 0$ of the cavity.

We define the expectation value of X_S:

$$\langle X_S(t)\rangle = \text{Tr}_S\{X_S\rho_S(t)\} = \text{Tr}\{X_S(t)\rho(t_0)\}, \tag{37}$$

where $\rho(t_0) = \rho_S(t_0)\otimes\rho_R(t_0)$ is the complete density operator and $\rho_S(t) = \text{Tr}_R\{U(t,t_0)\rho(t_0)U^\dagger(t,t_0)\}$ is the reduced density operator describing $\mathcal{S}$ with partial trace $\text{Tr}_R\{\cdot\}$ eliminating the degrees of freedom corresponding to its subscript.

We here assume that the reservoir is initially a vacuum state $\rho_R(t_0) \equiv |\emptyset\rangle\langle\emptyset|$ such that $\mathcal{D}^\dagger_{\text{in},t}(\cdot)$ cancels out in averaging. Finally, averaging Eq. (35), we find the master equation of Lindblad form for $\rho_S(t)$:

$$\frac{d}{dt}\rho_S(t) = -\frac{i}{\hbar}[H_S(t), \rho_S(t)] + \Gamma_c\left(c\rho_S(t)c^\dagger - \frac{1}{2}\{c^\dagger c, \rho_S(t)\}\right). \tag{38}$$

Here, all system operators σ, c are time independent (Schrödinger picture), and the remaining time dependence of $H_S(t)$ is due to the driving field $\Omega(t)$.

III. PRODUCTION OF A SINGLE PHOTON BY A DRIVEN ATOM TRAPPED IN A CAVITY

As an application, we derive from the preceding analysis a model for the generation of a single photon using a leaking cavity containing one atom driven by a pulsed laser of Rabi frequency $\Omega(t)$. The production of a single photon in such a system has been demonstrated with an atom flying through the cavity in a resonant stimulated Raman adiabatic passage configuration [42,43,73] and for a trapped ion in a cavity [74]. We next show that a large cavity detuning and an effective weak coupling regime allow direct and simple control of the photon shape.

A. The model

Since the system of interest involves only the atom and the cavity, in the effective model, the basis introduced in the inside-outside representation reduces to $\{|g,\emptyset\rangle, |e,\emptyset\rangle, |f,1\rangle, |f,\emptyset\rangle\}$ (see Fig. 2), where the third label is dropped due to the elimination of the reservoir degrees of freedom and the label "in" is omitted. Such dynamics involves the Lindblad equation derived previously (we omit the subscript S for ρ):

$$\frac{d}{dt}\rho(t) = -\frac{i}{\hbar}[H_S(t), \rho(t)] + \mathcal{L}[\rho(t)], \tag{39}$$

with the dissipator $\mathcal{L}[\rho] = \Gamma_c(c\rho c^\dagger - \frac{1}{2}\{\rho, c^\dagger c\})$. Equation (39) can be rewritten as

$$\frac{d}{dt}\rho(t) = -\frac{i}{\hbar}(\tilde{H}(t)\rho(t) - \rho(t)\tilde{H}^\dagger(t)) + \Gamma_c\, c\rho(t)c^\dagger, \tag{40}$$

where we introduced an anti-Hermitian dissipative Hamiltonian $\tilde{H}(t) = H_S(t) - i\hbar\frac{\Gamma_c}{2}c^\dagger c$, equivalent to (8). Expressing the Hamiltonian in a matrix form

$$H_S(t) = \hbar\begin{bmatrix}\mathbf{A}(t) & [0]_{3\times1}\\ [0]_{1\times3} & -\omega_c\end{bmatrix}, \tag{41a}$$

$$\mathbf{A}(t) = \begin{bmatrix}0 & \Omega(t) & 0\\ \Omega(t) & \Delta & g\\ 0 & g & 0\end{bmatrix} \tag{41b}$$

shows two decoupled dynamical blocks, $\mathbf{A}(t)$ and $\{-\omega_c\}$. From the density matrix

$$\rho(t) = \begin{bmatrix}\rho_{\mathbf{AA}}(t) & \rho_{\mathbf{A}0}(t)\\ \rho_{0\mathbf{A}}(t) & \rho_{00}(t)\end{bmatrix}, \tag{42}$$

we split Eq. (40) into two equations:

$$\dot{\rho}_{\mathbf{AA}} = -i(\tilde{\mathbf{A}}(t)\rho_{\mathbf{AA}}(t) - \rho_{\mathbf{AA}}(t)\tilde{\mathbf{A}}^\dagger(t)), \tag{43a}$$

$$\dot{\rho}_{00} = \Gamma_c\mathbf{D}\rho_{\mathbf{AA}}(t)\mathbf{D}^\dagger, \tag{43b}$$

where $\mathbf{D} = [0,0,1]$ is a block from the matrix representation $\mathbf{c}$ of the annihilation operator c, $\tilde{\mathbf{A}}(t) = \mathbf{A}(t) - \frac{i}{2}\Gamma_c\mathbf{D}^\dagger\mathbf{D}$. Choosing the initial condition in $|g,\emptyset\rangle$ makes the dynamics not involve ρ_{A0}, and Eq. (43a) corresponds thus to a Schrödinger equation with losses (i.e., with a non-Hermitian Hamiltonian) derived in Eq. (16), i.e., $\text{Tr}\rho_{AA} < 1$:

$$i\frac{\partial}{\partial t}|\psi_{\text{eff}}\rangle = \begin{bmatrix}0 & \Omega(t) & 0\\ \Omega(t) & \Delta & g\\ 0 & g & -i\frac{\Gamma_c}{2}\end{bmatrix}|\psi_{\text{eff}}\rangle \tag{44}$$

with ψ_{eff} being the state in the pseudomode picture. The population lost from the subspace spanned by the states $\{|g,\emptyset\rangle, |e,\emptyset\rangle, |f,1\rangle\}$ (on which the block $\mathbf{A}$ is defined) is

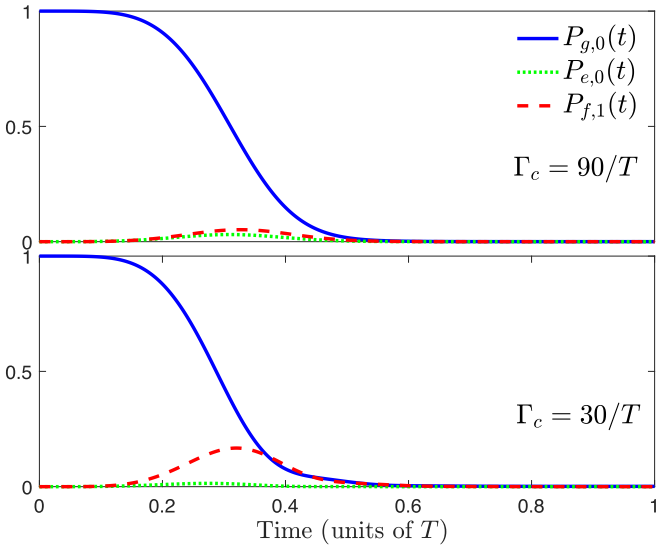

FIG. 5. Dynamics corresponding to Eq. (44) for cavities with different Γ_c factors. The system parameters are $\Omega(t) = \Omega_0 \sin^2(\frac{\pi t}{T})$, $(|g|, \Delta, \Omega_0, \omega_c) \times T = (60, 150, 60, 2416)$. As we can see from the figure, the stronger the leakage of the cavity is, the less the state $P_{f,1}$ is populated.

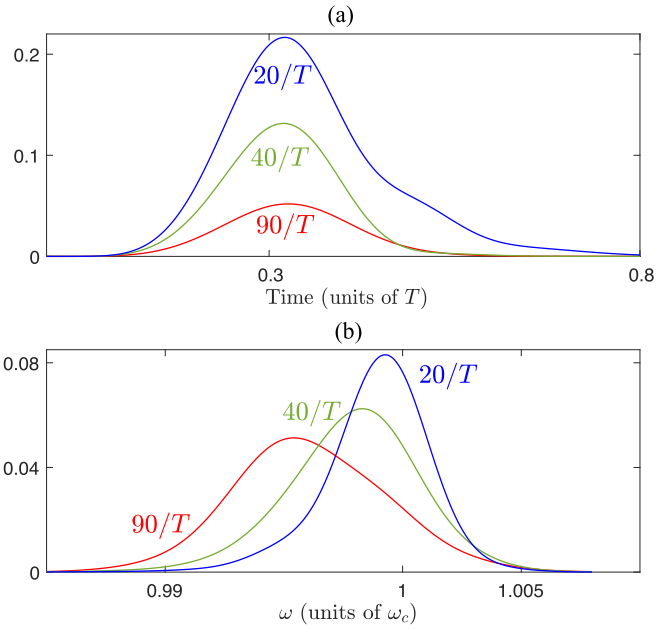

FIG. 6. Produced single-photon shape in the time (a) and frequency (b) domains for different values of the cavity decay rate Γ_c. The other parameters are the same as in Fig. 5.

collected in state $|f, \emptyset\rangle$ (on which the block $\{-\omega_c\}$ is defined), so that the whole system is closed: $P_{g,0}(t) + P_{e,0}(t) + P_{f,1}(t) + P_{f,0}(t) = 1$ with the population $P_{i,n}(t) = \langle i, n|\rho(t)|i, n\rangle = |c_{i,n}|^2$. We highlight that Eq. (44) is obtained from the inside-outside picture, for the cavity of mode c. This equation coincides with Eq. (16), obtained from pseudomode picture; hence in this limit the modes c and a are the same.

Rewriting (43b), we get

$$\frac{d}{dt}P_{f,0}(t) = \Gamma_c P_{f,1}(t). \tag{45}$$

On the other hand, from the definition of the average $\langle \mathcal{O} \rangle = \mathrm{Tr}(\rho\mathcal{O})$, one can write the photon flux (34) in terms of the populations:

$$\Phi(t) \equiv \frac{dn(t)}{dt} = \Gamma_c P_{f,1}(t). \tag{46}$$

We can then identify $P_{f,0}(t)$ as the number of outgoing photons: $P_{f,0}(t) \equiv n(t)$. The scheme enables us to derive the shape of the leaking photon, through its flux $\Phi(t)$ from the atom-cavity dynamics, which is determined by the Schrödinger equation (44).

B. The scheme for a large detuning

Here we start by analyzing the dynamics for different coupling regimes for a single-mode cavity ($L = L_0$). We compare the strong coupling regime $g > \Gamma_c$ with an intermediate coupling regime $g \lesssim \Gamma_c$. The parameters are chosen such that the approximate models described in Sec. II remain valid. Particular cases for intermediate and strong coupling regimes are presented in Fig. 5. As expected, in the strong coupling regime the single-photon state inside the cavity is more populated than the one in an intermediate coupling regime. In Fig. 6, we study cavities with different decay rates and analyze the produced photon inside and outside the cavity, using the full inside-outside representation [Eq. (19)]. In Fig. 6(a) the produced photon inside the cavity is presented ($P_{f,1}$). As one would expect, with the decrease in Γ_c the probability of the photon state inside the cavity increases. We also notice that for the given symmetric $\Omega(t)$ the shape of the photon takes an asymmetric form with the decrease in Γ_c. Figure 6(b) shows the shape of the leaked photon in the frequency domain ($P_{p,\mathrm{out}}$). As we can see from the figure, the better the quality of the cavity is, the more the leaked photon is centered around the cavity resonance frequency. As expected, the bandwidth of the photon gets narrower with the decrease in Γ_c.

The direct control of production of the shape of a single leaking photon can be achieved for a large detuning $\Delta \gg \Omega, g$ (allowing the adiabatic elimination of the excited state $|e, \emptyset\rangle$ [75]) and an effective weak coupling regime: $\Gamma_c \gg G, g^2/\Delta$ with $G = -g\Omega/\Delta$ being the (assumed positive) effective Raman coupling [allowing the adiabatic elimination of the state $|f, 1\rangle$ (Fig. 5)].

The adiabatic eliminations lead to

$$c_{g,0}(t) = e^{i\zeta(t)}e^{-\frac{\theta(t)}{2}}, \tag{47a}$$

$$\zeta(t) = \int_{t_i}^{t} dt' \frac{\Omega^2(t')}{\Delta}, \tag{47b}$$

$$\theta(t) = \int_{t_i}^{t} dt' \frac{4G^2(t')}{\Gamma_c}. \tag{47c}$$

We denote the initial time $t_i = 0$. From $c_{g,0}(t)$, i.e., for given g, Δ, and $\Omega(t)$, one can infer $c_{f,1}(t) = -i2(G(t)/\Gamma_c)c_{g,0,0}(t)$, and Eq. (46) then gives the shape of the photon flux:

$$\Phi(t) = \dot{\theta}(t)e^{-\theta(t)}. \tag{48}$$

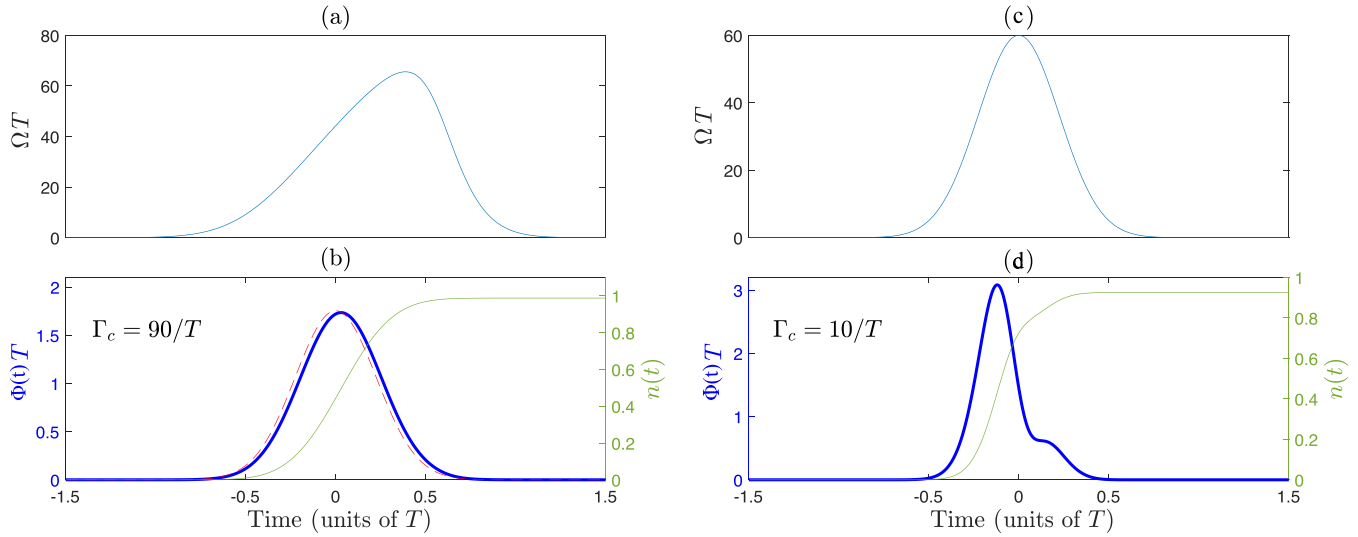

FIG. 7. (a) and (b) Rabi frequency $\Omega(t)T$ (50) with $(|g|, \Gamma_c, \Delta) \times T = (60, 90, 300)$, $\eta = 0.99$, determined from the desired Gaussian shape flux $\Phi(t)$ (51) [desired (dashed line) and numerically determined from the original model (44) (thick line)] of the single photon through the semitransparent mirror (in units of T); number of outgoing photons $n = \int_{-\infty}^{t} dt' \Phi(t') = \Gamma_c \int_{-\infty}^{t} dt' |c_{f,1}(t')|^2$ during the process (thin line). (c) and (d) Same as (a) and (b) but for $\Gamma_c = 10/T$ and a chosen Gaussian Rabi frequency $\Omega(t) = 60 \exp[-(\pi t/T)^2]/T$.

The inverse calculation allows one to tailor a desired photon flux by deriving explicitly the corresponding $\Omega(t)$ (for given g and Δ). This is achieved by determining $\theta(t)$ from (48):

$$\theta(t) = -\ln\left[1 - \int_0^t dt' \Phi(t')\right]. \tag{49}$$

We get the simple expression for the Rabi frequency by deriving this latter equation and from (47c):

$$\Omega(t) = \frac{\Delta\sqrt{\Gamma_c}}{2g}\sqrt{\frac{\Phi(t)}{1 - \int_0^t dt' \Phi(t')}}. \tag{50}$$

We remark that this definition of the Rabi frequency can diverge at large time. To prevent this, we introduce an efficiency parameter $\eta < 1$ which will ensure that $\Omega(t \to +\infty) = 0$ when $\Phi(t \to +\infty) = 0$ [42,43].

Numerical results for a chosen Gaussian probability for the single-photon shape

$$\Phi(t) = \frac{\eta\sqrt{\pi}}{T} e^{-\left(\frac{\pi t}{T}\right)^2}, \quad \int_{-\infty}^{+\infty} \Phi(t) dt = \eta, \tag{51}$$

are shown in Figs. 7(a) and 7(b). Using $\Gamma_c = 90/T$, we obtain $\max_t G(t) \approx 13/T \ll \Gamma_c$. We have also checked numerically the resulting flux by determining it from the numerical solution of the Schrödinger equation (44) (without considering the adiabatic elimination) with the Rabi frequency (50). The derived photon flux closely follows the desired shape as expected.

Other, more complex forms can be investigated through (50) [76–78], such as the ones obtained by the resonant process with flying atoms in Refs. [42,43].

Figures 7(c) and 7(d) show a different situation with a cavity of better effective quality: $\Gamma_c = 10/T$ and $\max_t G(t) = 12/T \approx \Gamma_c$, where the second adiabatic elimination cannot be made. In this case, the leakage of the photon occurs earlier and faster due to the earlier peak of the coupling. The smaller decay rate of the cavity leads to a deformation of the tail of the photonic shape.

IV. CONCLUSION

We have derived and analyzed models for the system of a Λ atom trapped in a cavity, featuring a semitransparent mirror and driven by laser pulses allowing the production of a single photon leaking out from the cavity. We introduced true-mode, inside-outside, and pseudomode representations for describing the system from first principles. From the exact modes of the system (the true-mode representation), we explicitly introduce the cavity-reservoir coupling, which allows one to describe the dynamics without any *a priori* approximations. We have demonstrated that under suitable approximations that we formulate, these different representations give accurate results that are similar to each other, yet generally differ. We particularly analyze a high-Q cavity scenario and show that this requirement alone, in general, is not enough for these approximate models to work. This is especially significant for the models where we consider cavities with higher losses and mode overlaps, namely, cavities with low refractive indices, such as plasmonic cavities. In nanophotonics, it is common to transpose these approximate models derived for optical cavities to plasmonic cavities. However, as shown here, these approximate models already yield different predictions for optical cavities with relatively high transmission.

In the literature, it is common to phenomenologically introduce the pseudomode representation. However, this kind of phenomenological approach does not provide the full description of the produced photon, namely, the outgoing photon shape in the frequency domain. In contrast, here, we recover the phenomenological model derived from first principles; moreover, it is complemented with the complete description of the system, including the full characteristics of the photon in the time domain as well as in the fre-

quency domain. This derivation justifies explicitly the Markov approximation producing an input-output relation from first principles via the nontrivial cavity-reservoir coupling (7). This allows a precise definition of the propagating outside photon state (24).

Finally, concepts, such as the Poynting vector, photon flux, input-output operators, and photon state, that characterize the propagation of the resulting leaking photons have been defined and connected: We have formulated an input-output relation taking into account the propagating effects, which allows a direct interpretation of the b_{out} operator through the Poynting vector and the photon flux. The generated flux is then determined from the quantum average of the dynamics of the photon number in the cavity, which results from a standard master equation that we have derived using the operators at $x = 0$. Different coupling regimes have been discussed. In particular, we have studied an effective weak coupling regime with a large detuning and a strong cavity leakage, such that the adiabatic elimination of the cavity state is performed. In this case, one can directly link the envelope of the driving field to the pulse shape of the outgoing single photon which can be tailored at will.

In order to demonstrate the concepts in a straightforward way, we have considered a simple model for the mirror, as a single layer with a fictitious large index. In practice, a large index is produced via a multilayer mirror. Such a (more realistic) model will be considered in future work. We will also take into account in a similar manner the reverse process of photon absorption and the full process of generation and absorption.

ACKNOWLEDGMENTS

We acknowledge H. Jauslin for helpful discussions. We acknowledge support from the European Union's Horizon 2020 research and innovation program under Marie Skłodowska-Curie Grant Agreement No. 765075 (LIMQUET). This research was also supported by the Ministry of Culture and Innovation and the National Research, Development and Innovation Office within the Quantum Information National Laboratory of Hungary (Grant No. 2022-2.1.1-NL-2022-00004).

APPENDIX A: INPUT-OUTPUT RELATION WITH THE USE OF A DIRAC DELTA DISTRIBUTION

In this Appendix, we show the mathematical inconsistency of the the standard development of the input-output relation (29) from the Heisenberg-Langevin equations (20) within the Markov approximation applied without a model for the coupling (see, e.g., Ref. [51]). By assuming a "flat" continuum via the approximation

$$\kappa_c(\omega) \approx \sqrt{\frac{\Gamma_c}{2\pi}} \tag{A1}$$

and pushing the ω integration from $-\infty$, we approximate the double integral in (25b) (considering for simplicity the case $x = 0$) as

$$\int_{t_0}^{t} dt' \int_{0}^{+\infty} d\omega \frac{|\kappa_c(\omega)|^2}{\sqrt{\Gamma_c}} c(t') e^{-i\omega(t-t')}$$

$$\approx \sqrt{\Gamma_c} \int_{t_0}^{t} dt' c(t') \int_{-\infty}^{+\infty} \frac{d\omega}{2\pi} e^{-i\omega(t-t')} \tag{A2a}$$

$$= \sqrt{\Gamma_c} \int_{t_0}^{t} dt' c(t') \delta(t-t') \tag{A2b}$$

$$= \frac{\sqrt{\Gamma_c}}{2} c(t). \tag{A2c}$$

The last step, which can be reformulated in a simpler case as

$$\int_{-\infty}^{0} dt\, c(t)\delta(t) = \frac{1}{2} c(0), \tag{A3}$$

is mathematically undefined. Since the distributions are defined on the real line via the integration on a test function, it indeed necessitates the introduction of a multiplication with the Heaviside distribution:

$$\int_{-\infty}^{+\infty} dt\, c(t) H(-t)\delta(t) = \int_{-\infty}^{0} dt\, c(t)\delta(t). \tag{A4}$$

However such a product of two nonregular distributions is undefined, here more specifically the product of the Dirac delta distribution with the Heaviside distribution of discontinuity localized where the Dirac delta is infinite. This has been analyzed in Ref. [79].

An explicit analysis can be conducted by defining a model for the Dirac delta distribution using a family of (noneven) functions represented in Fig. 8,

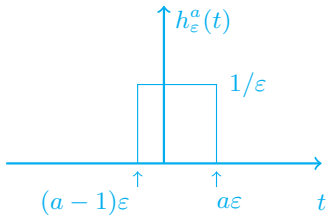

FIG. 8. Representation of a family of noneven functions parametrized by a real number $0 < a < 1$ tending to the Dirac delta distribution in the limit $\epsilon \to 0$.

$$h^a_\epsilon(t) = \begin{cases} 0 & \text{for } t < (a-1)\epsilon \\ 1/\epsilon & \text{for } (a-1)\epsilon \leqslant t \leqslant a\epsilon \\ 0 & \text{for } t > a\epsilon, \end{cases} \tag{A5}$$

parametrized by a real number $0 < a < 1$, in the limit $\epsilon \to 0$. We can indeed check that they satisfy the Dirac delta distribution [applied on a test function $\varphi(t)$]:

$$\lim_{\epsilon\to 0} \int_{-\infty}^{+\infty} dt\, \varphi(t) h^a_\epsilon(t) = \lim_{\epsilon\to 0} \frac{1}{\epsilon} \int_{(a-1)\epsilon}^{a\epsilon} dt\, \varphi(t)$$

$$= \lim_{\epsilon\to 0} \int_{a-1}^{a} ds\, \varphi(\epsilon s)$$

$$= \varphi(0), \tag{A6}$$

where we have applied the change of variable $s = t/\epsilon$. We note that the limit $\epsilon \to 0$ guarantees that $\delta(t) = \lim_{\epsilon\to 0} h^a_\epsilon(t)$ is an even distribution.

Applying this model on (A3), we obtain

$$\begin{aligned}\lim_{\epsilon\to 0}\int_{-\infty}^{0} dt\, c(t)h^a_\epsilon(t) &= \lim_{\epsilon\to 0}\frac{1}{\epsilon}\int_{(a-1)\epsilon}^{0} dt\, c(t)\\ &= \lim_{\epsilon\to 0}\int_{a-1}^{0} ds\, c(\epsilon s)\\ &= (1-a)c(0). \end{aligned} \tag{A7}$$

This shows that the result depends on the details of the model of the Dirac delta distribution [80]. We recover the result of (A3) only for a particular even-function model (i.e., $a = 1/2$).

As a consequence, the derivation (A2) is not valid in general. It necessitates a specific model for the coupling $\kappa_c(\omega)$, as considered from first principles in this paper.

APPENDIX B: LORENTZIAN STRUCTURE OF THE CAVITY RESPONSE FUNCTION

As shown in Refs. [27,57,61], for a one-dimensional, single-layer dielectric cavity, having a perfect mirror placed at $x = -L$ and a semitransparent mirror at $x = 0$, the response function and the quantized electric field inside the cavity are written as follows:

$$T(\omega) = \frac{t(\omega)}{1 + r(\omega)e^{2i\frac{\omega}{c}(L+\frac{\delta}{2})}}, \tag{B1}$$

$$\begin{aligned}E_{\text{in}}(x) = \int_0^\infty d\omega \sqrt{\frac{\hbar\omega}{\pi c\mathcal{A}\epsilon_0}}\sin\left[\frac{\omega}{c}(x+L)\right]e^{i\frac{\omega}{c}L}T(\omega)a_\omega,\\ + \text{H.c.},\end{aligned} \tag{B2}$$

where $t(\omega)$ and $r(\omega)$ are single-layer spectral transmission and reflection functions,

$$|t(\omega)|^2 + |r(\omega)|^2 = 1, \tag{B3}$$

$$t(\omega)r^*(\omega) + t^*(\omega)r(\omega) = 0, \tag{B4}$$

with

$$t(\omega) = \frac{(1-r^2)e^{i(n-1)\frac{\omega}{c}\delta}}{1 - e^{2in\frac{\omega}{c}\delta}r^2}, \tag{B5}$$

$$r(\omega) = e^{-i\frac{\omega}{c}\delta}\frac{r\left(e^{2in\frac{\omega}{c}\delta} - 1\right)}{1 - e^{2in\frac{\omega}{c}\delta}r^2} = |r(\omega)|e^{i\phi_r(\omega)}, \tag{B6}$$

and $r = \frac{n-1}{n+1}$ is the reflectivity of the mirror with thickness $\delta = \frac{\lambda_c}{4n}$, λ_c being the cavity resonance wavelength. It can be shown [27,57,61] that this response function can be written as a sum of Lorentzian-like functions, for a cavity with a low transmission rate:

$$|T(\omega)|^2 \approx \sum_m \frac{c}{2L}\frac{\Gamma_m}{(\omega-\omega_m)^2 + \left(\frac{\Gamma_m}{2}\right)^2}, \tag{B7}$$

where

$$\Gamma_m = -\frac{c}{L}\ln|r(\omega_m)|, \tag{B8}$$

$$\omega_m = m\frac{\pi c}{L} + \frac{c}{2L}(\pi - \phi_r(\omega_m)). \tag{B9}$$

For a high-Q cavity with a low transmission rate [$|t(\omega)| \approx |\underline{t}| \ll 1, \phi_r(\omega_m) \approx \pi$], each Lorentzian of the sum (B7) is well separated from the others ($\Gamma_m \ll \pi c/L$), and we can deduce the following:

$$T(\omega) = \sum_m \sqrt{\frac{c}{2L}}\frac{\sqrt{\Gamma_m}}{\omega - \omega_m + i\frac{\Gamma_m}{2}}. \tag{B10}$$

With (B2) one can write the atom-environment interaction Hamiltonian from the dipole approximation [27]: $H_{\text{int}} = -dE_{\text{in}}$, which, using the expression (B10), leads to the single-mode coupling function of the form (3b).

APPENDIX C: DISCRETIZATION OF THE CONTINUOUS INTEGRALS

Equations (13) and (19) are integrated numerically via discretizing the continuum. In order to perform discretization properly, we analyze the continuous parts of the states (11) and (18), where the photon states $|1_\omega\rangle$ and $|1_{\omega,\text{out}}\rangle$ and the coefficients $\tilde{c}_{f,1}(\omega,t)$ and $c_{f,0,1}(\omega,t)$ all have units of $1/\sqrt{\omega}$, making the corresponding integrals dimensionless. Thus we can do the following discretization:

$$\int_0^\infty d\omega\, \tilde{c}_{f,1}(\omega,t)|\mathbf{1}_\omega\rangle = \sum_{i=1}^{m}\sqrt{d\omega}\tilde{c}_{f,1}(\omega_i,t)\sqrt{d\omega}|\mathbf{1}_{\omega_i}\rangle,$$

$$\int_0^\infty d\omega\, c_{f,0,1}(\omega,t)|1_{\omega,\text{out}}\rangle = \sum_{i=1}^{m}\sqrt{d\omega}c_{f,0,1}(\omega_i,t)\sqrt{d\omega}|1_{\omega_i,\text{out}}\rangle,$$

where $d\omega$ is the step of the discretization. By denoting the dimensionless quantities of the sum as $\tilde{\mathbf{c}}_{f,1}(\omega_i,t) = \sqrt{d\omega}\,\tilde{c}_{f,1}(\omega_i,t)$, $|\tilde{\mathbf{1}}_{\omega_i}\rangle = \sqrt{d\omega}|\mathbf{1}_{\omega_i}\rangle$ and $\mathbf{c}_{f,0,1}(\omega_i,t) = \sqrt{d\omega}\,c_{f,0,1}(\omega_i,t)$, $|\mathbf{1}_{\omega_i,\text{out}}\rangle = \sqrt{d\omega}|1_{\omega_i,\text{out}}\rangle$, we can calculate the probability amplitudes of finding the photon in states $|\tilde{\mathbf{1}}_{\omega_i}\rangle$ and $|\mathbf{1}_{\omega_i,\text{out}}\rangle$, respectively:

$$\tilde{P}(\omega_i,t) = |\langle\tilde{\mathbf{1}}_{\omega_i}|\tilde{\psi}\rangle|^2 = |\tilde{\mathbf{c}}_{f,1}(\omega_i,t)|^2,$$

$$P(\omega_i,t) = |\langle\mathbf{1}_{\omega_i,\text{out}}|\psi\rangle|^2 = |\mathbf{c}_{f,0,1}(\omega_i,t)|^2.$$

Taking this discretization into account, in Eq. (13), the discretization of the function $\eta(\omega)$ becomes $\sqrt{d\omega}\,\eta(\omega_1), \sqrt{d\omega}\,\eta(\omega_2), \ldots, \sqrt{d\omega}\,\eta(\omega_m)$, and the equations become

$$\begin{aligned}i\dot{\tilde{c}}_{g,0}(t) &= \Omega\,\tilde{c}_{e,0}(t),\\ i\dot{\tilde{c}}_{e,0}(t) &= \Delta\,\tilde{c}_{e,0}(t) + \Omega\,\tilde{c}_{g,0}(t) + i\sum_m \tilde{\eta}_{\omega_m}\tilde{\mathbf{c}}_{f,1}(\omega_m,t),\\ i\dot{\tilde{\mathbf{c}}}_{f,1}(\omega_1,t) &= (\Delta - \Delta_c + \omega_1 - \omega_c)\tilde{\mathbf{c}}_{f,1}(\omega_1,t) - i\tilde{\eta}^*_{\omega_1}\tilde{c}_{e,0}(t),\\ &\vdots\\ i\dot{\tilde{\mathbf{c}}}_{f,1}(\omega_m,t) &= (\Delta - \Delta_c + \omega_m - \omega_c)\tilde{\mathbf{c}}_{f,1}(\omega_m,t) - i\tilde{\eta}^*_{\omega_m}\tilde{c}_{e,0}(t),\end{aligned}$$

with $\tilde{\eta}_{\omega_m} = \sqrt{d\omega}\,\eta(\omega_m)$.

Similarly, Eq. (19) becomes

$$\begin{aligned}
i\dot{c}_{g,0}(t) &= \Omega\, c_{e,0}(t),\\
i\dot{c}_{e,0}(t) &= \Delta\, c_{e,0}(t) + \Omega\, c_{g,0}(t) + g\, c_{f,1,0}(t),\\
i\dot{c}_{f,1,0}(t) &= (\Delta - \Delta_c) c_{f,1,0} + g\, c_{e,0}(t)\\
&\quad - i\sum_m \tilde{\kappa}_c^*(\omega_m)\, \mathbf{c}_{f,0,1}(\omega_m, t),\\
i\dot{\mathbf{c}}_{f,0,1}(\omega_1, t) &= (\Delta - \Delta_c + \omega_1 - \omega_c)\mathbf{c}_{f,0,1}(\omega_1, t)\\
&\quad + i\tilde{\kappa}_c(\omega_1)\, c_{f,1,0}(t),\\
&\vdots\\
i\dot{\mathbf{c}}_{f,0,1}(\omega_m, t) &= (\Delta - \Delta_c + \omega_m - \omega_c)\mathbf{c}_{f,0,1}(\omega_m, t)\\
&\quad + i\tilde{\kappa}_c(\omega_m)\, c_{f,1,0}(t),
\end{aligned}$$

where $\tilde{\kappa}_c(\omega_m) = \sqrt{d\omega}\,\kappa_c(\omega_m)$.

By solving these systems of equations numerically using a sufficiently large number of (typically 100 000) states discretizing the continuum, we obtain the solutions presented in Fig. 3.

APPENDIX D: POYNTING VECTOR DERIVATION

Following the definition of the Poynting vector [57,62], we can write it in the true-mode representation, using the modes derived for the outside of the cavity [27,57,61]:

$$S(x) = -\frac{1}{2\mu_0}(B_{\text{out}}(x)E_{\text{out}}(x) + E_{\text{out}}(x)B_{\text{out}}(x)),$$

where $\mu_0 = 1/(c^2\epsilon_0)$ is the vacuum permeability and

$$E_{\text{out}}(x) = -\frac{i}{\sqrt{2\pi c\mathcal{A}}}\int_0^\infty d\omega \sqrt{\frac{\hbar\omega}{2\epsilon_0}}((R_\omega e^{i\frac{\omega}{c}x} - e^{-i\frac{\omega}{c}x})a_\omega - \text{H.c.}),$$

$$B_{\text{out}}(x) = \frac{i}{c\sqrt{2\pi c\mathcal{A}}}\int_0^\infty d\omega \sqrt{\frac{\hbar\omega}{2\epsilon_0}}((R_\omega e^{i\frac{\omega}{c}x} + e^{-i\frac{\omega}{c}x})a_\omega - \text{H.c.}),$$

with

$$R_\omega = e^{2i\frac{\omega}{c}L}\frac{T(\omega)}{T^*(\omega)} \approx \sqrt{\frac{2\pi}{\Gamma_c}}\sqrt{\frac{\omega_c}{\omega}}\alpha^*(\omega)\left(\omega - \omega_c - i\frac{\Gamma_c}{2}\right).$$

$\alpha(\omega)$ is the coefficient linking the true mode a_ω to the discrete cavity mode c: $a_\omega = \alpha(\omega)c + \int_0^\infty d\omega'\beta(\omega,\omega')b_{\omega'}$. It can be written as follows [57]:

$$\alpha(\omega) = \sqrt{\frac{\omega}{\omega_c}}\sqrt{\frac{L}{\pi c}}\,\text{sinc}\left((\omega - \omega_c)\frac{L}{c}\right)e^{-i\frac{\omega}{c}L}T^*(\omega).$$

Taking these into account, we get the following Poynting vector, for the propagation in the positive x direction:

$$S(x) = \frac{\hbar}{2\pi\mathcal{A}}\int_0^\infty d\omega d\omega' \sqrt{\omega\omega'}\,\text{Re}\{R_\omega R_{\omega'}^* e^{i\frac{(\omega-\omega')}{c}x} a_{\omega'}^\dagger a_\omega\}.$$

Furthermore, by writing a_ω in terms of the outside operator corresponding to the inside-outside representation, $a_\omega = \int d\omega'\beta(\omega,\omega')b_{\omega'}$, and recalling that $i\int d\omega d\omega'\omega\alpha^*(\omega)\beta(\omega,\omega')b_{\omega'} = \int d\omega\kappa_c^*(\omega)b_\omega$ [57], we obtain the following:

$$S(x) = \frac{\hbar}{\mathcal{A}}\frac{\omega_c}{\Gamma_c}\int_0^\infty d\omega d\omega' \kappa_c^*(\omega)\kappa_c(\omega')e^{i\frac{(\omega-\omega')}{c}x} b_{\omega'}^\dagger b_\omega.$$

Via defining the integrated reservoir operator as

$$b(x) = \frac{1}{\sqrt{\Gamma_c}}\int_0^\infty d\omega \kappa_c^*(\omega)e^{i\frac{\omega}{c}x}b_\omega, \tag{D1}$$

the expression for the Poynting vector becomes

$$S(x) = \frac{\hbar}{\mathcal{A}}\frac{\omega_c}{\Gamma_c}b^\dagger(x)b(x). \tag{D2}$$

APPENDIX E: EVALUATION OF THE INTEGRAL (25b)

In order to evaluate the integral in (25b), we use the following expression for $\kappa_c(\omega)$:

$$\kappa_c(\omega) = \sqrt{\frac{\Gamma_c}{2\pi}}e^{-i\frac{\omega}{c}L}\text{sinc}\left((\omega - \omega_c)\frac{L}{c}\right).$$

We calculate the following integral:

$$\begin{aligned}
\int_0^\infty d\omega\, |\kappa_c(\omega)|^2 e^{-i\omega\tau} &= \frac{\Gamma_c}{2\pi}\left(\frac{c}{L}\right)^2\\
&\quad \times \int_0^\infty d\omega\, \frac{\sin^2\left((\omega-\omega_c)\frac{L}{c}\right)}{(\omega-\omega_c)^2}e^{-i\omega\tau},
\end{aligned} \tag{E1}$$

where $\tau = t - t' - \frac{x}{c}$. This leads to the evaluation of the integral of the following form (since $\omega_c = \frac{\pi c}{L}$, this is significantly larger than $\frac{c}{L}$, such that the integral can be evaluated as $\int_0^\infty \to \int_{-\infty}^\infty$):

$$\int_{-\infty}^\infty dx\, \frac{e^{\pm ix\tau}}{x^2}.$$

This integral can be evaluated in the complex plane, and its value is different for negative and positive parameters τ. Taking this into account, it can be shown that the integral in (E1) becomes

$$\begin{aligned}
&\frac{\Gamma_c}{2\pi}\left(\frac{c}{L}\right)^2\frac{1}{2}e^{-i\omega_c(t-t'-\frac{x}{c})}\\
&\times\begin{cases}
0, & t' > t - \frac{x}{c} + \frac{2L}{c}\\
-\pi\left(t' - t + \frac{x}{c} - \frac{2L}{c}\right), & t - \frac{x}{c} < t' < t - \frac{x}{c} + \frac{2L}{c}\\
\pi\left(t' - t + \frac{x}{c} + \frac{2L}{c}\right), & t - \frac{x}{c} - \frac{2L}{c} < t' < t - \frac{x}{c}\\
0, & t' < t - \frac{x}{c} - \frac{2L}{c}.
\end{cases}
\end{aligned} \tag{E2}$$

Having calculated the integral over the frequency, we can now evaluate the time integral in (25b). Taking into account the

results in (E2), we can reduce the integration range to the following ones:

$$\int_{t_0}^{t} = \int_{t-\frac{x}{c}-\frac{2L}{c}}^{t-\frac{x}{c}} + \int_{t-\frac{x}{c}}^{t-\frac{x}{c}+\frac{2L}{c}}, \quad \text{when } x > 2L,$$

$$\int_{t_0}^{t} = \int_{t-\frac{x}{c}-\frac{2L}{c}}^{t-\frac{x}{c}} + \int_{t-\frac{x}{c}}^{t}, \quad \text{when } 0 < x < 2L$$

with $t > t_0 + \frac{x}{c} + \frac{2L}{c}$. Considering that we analyze the dynamics for times much bigger than the round trip time of the produced photon, i.e., $t \gg \frac{2L}{c}$ (coarse-grained approximation), the integral for the case $x < 2L$ can be evaluated the same way as the integral for $x > 2L$, since $t + 2L/c > t - x/c + 2L/c \approx t$. Hence the integrals above can be evaluated as follows:

$$\int_{t-\frac{x}{c}}^{t-\frac{x}{c}+\frac{2L}{c}} dt' f(t') = \frac{1}{2}\left[f\left(t - \frac{x}{c} + \frac{2L}{c}\right) + f\left(t - \frac{x}{c}\right)\right]\frac{2L}{c},$$

$$\int_{t-\frac{x}{c}-\frac{2L}{c}}^{t-\frac{x}{c}} dt' f(t') = \frac{1}{2}\left[f\left(t - \frac{x}{c} - \frac{2L}{c}\right) + f\left(t - \frac{x}{c}\right)\right]\frac{2L}{c}.$$

Hence, for the full integral, we obtain

$$\int_{t_0}^{t} dt' \int_0^{\infty} d\omega\, |\kappa_c(\omega)|^2 e^{-i\omega(t-t'-\frac{x}{c})} c(t') = \Gamma_c c\left(t - \frac{x}{c}\right).$$

For the case $x = 0$, the integration over the frequency in (E1) gives the following result:

$$\frac{\Gamma_c}{2\pi}\left(\frac{c}{L}\right)^2 \frac{1}{2} e^{-i\omega_c(t-t')} \times \begin{cases} 0, & t' > \frac{2L}{c} \\ -\pi\left(t' - t + \frac{x}{c} - \frac{2L}{c}\right), & t < t' < t + \frac{2L}{c} \\ \pi\left(t' - t + \frac{x}{c} + \frac{2L}{c}\right), & t - \frac{2L}{c} < t' < t \\ 0, & t' < t - \frac{2L}{c}. \end{cases} \tag{E3}$$

Since the upper limit of the time integration is t, the second line of (E3) does not contribute to the integration over the time, and the overall integral becomes

$$\int_{t_0}^{t} dt' \int_0^{\infty} d\omega\, |\kappa_c(\omega)|^2 e^{-i\omega(t-t')} c(t') = \frac{\Gamma_c}{2} c(t).$$

APPENDIX F: DERIVATION OF THE MASTER EQUATION

In the following, we derive the dynamics of $X_S(t)$ from the Heisenberg equation, using Eqs. (4) and (36):

$$\begin{aligned} \frac{d}{dt}X_S(t) = -\frac{i}{\hbar}[X_S(t), H^{(H)}(t)] &= -\frac{i}{\hbar}\left[X_S(t), H_S^{(H)}(t)\right] \\ &+ \int_0^{\infty} d\omega (\kappa_c(\omega) b_\omega^\dagger(t)[X_S(t), c(t)] \\ &- \kappa_c^*(\omega)[X_S(t), c^\dagger(t)] b_\omega(t)). \end{aligned} \tag{F1}$$

From the definition (25a), we have $\int_0^{\infty} d\omega\, \kappa_c^*(\omega) b_\omega(t) = \sqrt{\Gamma_c} b(x = 0, t)$, for which we can use the relation (30); hence

$$\begin{aligned} \frac{d}{dt}X_S(t) &= -\frac{i}{\hbar}\left[X_S(t), H_S^{(H)}(t)\right] + \left(\sqrt{\Gamma_c} b_{\text{in}}^\dagger(t) + \frac{\Gamma_c}{2} c^\dagger(t)\right)[X_S(t), c(t)] - [X_S(t), c^\dagger(t)]\left(\sqrt{\Gamma_c} b_{\text{in}}(t) + \frac{\Gamma_c}{2} c(t)\right) \\ &= -\frac{i}{\hbar}\left[X_S(t), H_S^{(H)}(t)\right] + \sqrt{\Gamma_c} b_{\text{in}}^\dagger(t)[X_S(t), c(t)] - [X_S(t), c^\dagger(t)]\sqrt{\Gamma_c} b_{\text{in}}(t) + \Gamma_c\left(c^\dagger(t) X_S(t) c(t) - \frac{1}{2}\{c^\dagger(t) c(t), X_S(t)\}\right). \end{aligned}$$

We further define the time-dependent dissipator $\mathcal{D}_{\text{in},t}^\dagger(X_S(t)) = \sqrt{\Gamma_c} b_{\text{in}}^\dagger(t)[X_S(t), c(t)] - [X_S(t), c^\dagger(t)]\sqrt{\Gamma_c}\, b_{\text{in}}(t)$, leading to

$$\begin{aligned} \frac{d}{dt}X_S(t) = -\frac{i}{\hbar}\left[X_S(t), H_S^{(H)}(t)\right] &+ \mathcal{D}_{\text{in},t}^\dagger(X_S(t)) \\ &+ \Gamma_c\left(c^\dagger(t) X_S(t) c(t) - \frac{1}{2}\{c^\dagger(t) c(t), X_S(t)\}\right). \end{aligned} \tag{F2}$$

The expectation value of X_S can be calculated as follows:

$$\begin{aligned} \langle X_S(t)\rangle &= \text{Tr}\{X_S(t)\rho(t_0)\} \\ &= \text{Tr}\{X_S U(t, t_0)\rho(t_0) U^\dagger(t, t_0)\} \\ &= \text{Tr}_S\{\text{Tr}_R\{X_S U(t, t_0)\rho(t_0) U^\dagger(t, t_0)\}\} \\ &= \text{Tr}_S\{X_S \rho_S(t)\}, \end{aligned}$$

where we have used the cyclic property of the trace and defined $\rho_S(t) = \text{Tr}_R\{U(t, t_0)\rho(t_0) U^\dagger(t, t_0)\}$. Similarly, using the property $\text{Tr}\{A + B\} = \text{Tr}\{A\} + \text{Tr}\{B\}, \forall A, B$, we can calculate the averages on the right-hand side of Eq. (F2):

$$\begin{aligned} \left\langle\left[X_S(t), H_S^{(H)}(t)\right]\right\rangle &= \text{Tr}\left\{\left[X_S(t), H_S^{(H)}(t)\right]\rho(t_0)\right\} \\ &= \text{Tr}\{[X_S, H_S(t)] U(t, t_0)\rho(t_0) U^\dagger(t, t_0)\} \\ &= \text{Tr}_S\{[X_S, H_S(t)]\rho_S(t)\} \\ &= \text{Tr}_S\{X_S[H_S(t), \rho_S(t)]\}, \\ \langle c^\dagger(t) X_S(t) c(t)\rangle &= \text{Tr}_S\{c^\dagger X_S c \rho_S(t)\} \\ &= \text{Tr}_S\{X_S c \rho_S(t) c^\dagger\}, \\ \langle\{c^\dagger(t) c(t), X_S(t)\}\rangle &= \text{Tr}_S\{\{c^\dagger c, X_S\}\rho_S(t)\} \\ &= \text{Tr}_S\{X_S\{\rho_S(t), c^\dagger c\}\}. \end{aligned}$$

Assuming that the reservoir is initially a vacuum state $\rho_R(t_0) = |\emptyset\rangle\langle\emptyset|$, for the dissipator part $\mathcal{D}^\dagger_{\text{in},t}$ we get

$$\begin{aligned}\text{Tr}\{b^\dagger_{\text{in}}(t)\ \ &[X_S(t), c(t)]\rho(t_0)\}\\ &= \text{Tr}\{[X_S(t), c(t)]\rho(t_0)b^\dagger_{\text{in}}(t)\}\\ &= \text{Tr}\{[X_S(t), c(t)]\rho_S(t_0)\otimes\rho_R(t_0)b^\dagger_{\text{in}}(t)\}\\ &= \text{Tr}\{[X_S(t), c(t)]\rho_S(t_0)\otimes|\emptyset\rangle\langle\emptyset|b^\dagger_{\text{in}}(t)\} = 0.\end{aligned}$$

Similarly,

$$\text{Tr}\{[X_S(t), c^\dagger(t)]b_{\text{in}}(t)\rho(t_0)\} = 0.$$

Finally, Eq. (F2) becomes

$$\begin{aligned}\text{Tr}_S\left\{X_S\frac{d\rho_S(t)}{dt}\right\} &= \text{Tr}_S\{X_S[H_S(t), \rho_S(t)]\}\\ &+ \Gamma_c\left(\text{Tr}_S\{X_S c\rho_S(t)c^\dagger\} - \frac{1}{2}\text{Tr}_S\{X_S\{\rho_S(t), c^\dagger c\}\}\right).\end{aligned}$$

Furthermore, using the property $\forall A$, $\text{Tr}\{AB\} = \text{Tr}\{AC\} \Leftrightarrow B = C$, we obtain the master equation for $\rho_S(t)$:

$$\frac{d}{dt}\rho_S(t) = [H_S(t), \rho_S(t)] + \Gamma_c\left(c\rho_S(t)c^\dagger - \frac{1}{2}\{\rho_S(t), c^\dagger c\}\right).$$

[1] M. A. Nielsen and I. L. Chuang, *Quantum Computation and Quantum Information* (Cambridge University Press, Cambridge, 2000).

[2] D. Bouwmeester, A. K. Ekert, and A. Zeilinger, *The Physics of Quantum Information: Quantum Cryptography, Quantum Teleportation, Quantum Computation*, 1st ed. (Springer, New York, 2010).

[3] A. S. Cacciapuoti, M. Caleffi, F. Tafuri, F. S. Cataliotti, S. Gherardini, and G. Bianchi, Quantum internet: Networking challenges in distributed quantum computing, IEEE Network **34**, 137 (2020).

[4] A. S. Cacciapuoti, M. Caleffi, R. Van Meter, and L. Hanzo, When entanglement meets classical communications: Quantum teleportation for the quantum internet, IEEE Trans. Commun. **68**, 3808 (2020).

[5] J. I. Cirac, P. Zoller, H. J. Kimble, and H. Mabuchi, Quantum State Transfer and Entanglement Distribution among Distant Nodes in a Quantum Network, Phys. Rev. Lett. **78**, 3221 (1997).

[6] H. J. Kimble, The quantum internet, Nature (London) **453**, 1023 (2008).

[7] J. I. Cirac and H. J. Kimble, Quantum optics, what next? Nat. Photonics **11**, 18 (2017).

[8] B. Lounis and M. Orrit, Single-photon sources, Rep. Prog. Phys. **68**, 1129 (2005).

[9] C. Santori, D. Fattal, and Y. Yamamoto, *Single-Photon Devices and Applications* (Wiley-VCH, New York, 2010).

[10] I. Bialynicki-Birula, V photon wave function, Prog. Opt. **36**, 245 (1996).

[11] J. E. Sipe, Photon wave functions, Phys. Rev. A **52**, 1875 (1995).

[12] B. J. Smith and M. G. Raymer, Photon wave functions, wave-packet quantization of light, and coherence theory, New J. Phys. **9**, 414 (2007).

[13] N. Gisin, G. Ribordy, W. Tittel, and H. Zbinden, Quantum cryptography, Rev. Mod. Phys. **74**, 145 (2002).

[14] N. Sangouard and H. Zbinden, What are single photons good for? J. Mod. Opt. **59**, 1458 (2012).

[15] T. D. Barrett, A. Rubenok, D. Stuart, O. Barter, A. Holleczek, J. Dilley, P. B. R. Nisbet-Jones, K. Poulios, G. D. Marshall, J. L. O'Brien, A. Politi, J. C. F. Matthews, and A. Kuhn, Multimode interferometry for entangling atoms in quantum networks, Quantum Sci. Technol. **4**, 025008 (2019).

[16] A. Gogyan, S. Guérin, and Y. Malakyan, Deterministic generation of high-dimensional entanglement between distant atomic memories via multiphoton exchange, Phys. Rev. A **103**, 062611 (2021).

[17] J.-T. Shen and S. Fan, Theory of single-photon transport in a single-mode waveguide. II. Coupling to a whispering-gallery resonator containing a two-level atom, Phys. Rev. A **79**, 023838 (2009).

[18] X. Maître, E. Hagley, G. Nogues, C. Wunderlich, P. Goy, M. Brune, J. M. Raimond, and S. Haroche, Quantum Memory with a Single Photon in a Cavity, Phys. Rev. Lett. **79**, 769 (1997).

[19] A. Kuhn, M. Hennrich, and G. Rempe, Deterministic Single-Photon Source for Distributed Quantum Networking, Phys. Rev. Lett. **89**, 067901 (2002).

[20] J. McKeever, A. Boca, A. D. Boozer, R. Miller, J. R. Buck, A. Kuzmich, and H. J. Kimble, Deterministic generation of single photons from one atom trapped in a cavity, Science **303**, 1992 (2004).

[21] T. Wilk, S. C. Webster, A. Kuhn, and G. Rempe, Single-atom single-photon quantum interface, Science **317**, 488 (2007).

[22] S. Ritter, C. Nölleke, C. Hahn, A. Reiserer, A. Neuzner, M. Uphoff, M. Mücke, E. Figueroa, J. Bochmann, and G. Rempe, An elementary quantum network of single atoms in optical cavities, Nature (London) **484**, 195 (2012).

[23] M. Mücke, J. Bochmann, C. Hahn, A. Neuzner, C. Nölleke, A. Reiserer, G. Rempe, and S. Ritter, Generation of single photons from an atom-cavity system, Phys. Rev. A **87**, 063805 (2013).

[24] A. D. Boozer, A. Boca, R. Miller, T. E. Northup, and H. J. Kimble, Reversible State Transfer between Light and a Single Trapped Atom, Phys. Rev. Lett. **98**, 193601 (2007).

[25] A. Kuhn and D. Ljunggren, Cavity-based single-photon sources, Contemp. Phys. **51**, 289 (2010).

[26] J. Dilley, P. Nisbet-Jones, B. W. Shore, and A. Kuhn, Single-photon absorption in coupled atom-cavity systems, Phys. Rev. A **85**, 023834 (2012).

[27] A. Saharyan, J.-R. Álvarez, T. H. Doherty, A. Kuhn, and S. Guérin, Light-matter interaction in open cavities with dielectric stacks, Appl. Phys. Lett. **118**, 154002 (2021).

[28] K. J. Vahala, Optical microcavities, Nature (London) **424**, 839 (2003).

[29] B. Dawson, N. Furtak-Wells, T. Mann, G. Jose, and A. Beige, Spontaneous emission of atomic dipoles near two-sided semi-transparent mirrors, in *Nanophotonics VIII, Proceedings of SPIE*, Vol. 11345, edited by D. L. Andrews, A. J. Bain,

M. Kauranen, and J.-M. Nunzi (International Society for Optics and Photonics, Bellingham, WA, 2020), pp. 85–90.
[30] N. Furtak-Wells, L. A. Clark, R. Purdy, and A. Beige, Quantizing the electromagnetic field near two-sided semitransparent mirrors, Phys. Rev. A **97**, 043827 (2018).
[31] A. V. Gorshkov, A. André, M. D. Lukin, and A. S. Sørensen, Photon storage in Λ-type optically dense atomic media. I. Cavity model, Phys. Rev. A **76**, 033804 (2007).
[32] K. S. Choi, H. Deng, J. Laurat, and H. J. Kimble, Mapping photonic entanglement into and out of a quantum memory, Nature (London) **452**, 67 (2008).
[33] M. Keller, B. Lange, K. Hayasaka, W. Lange, and H. Walther, Continuous generation of single photons with controlled waveform in an ion-trap cavity system, Nature (London) **431**, 1075 (2004).
[34] N. Piro, F. Rohde, C. Schuck, M. Almendros, J. Huwer, J. Ghosh, A. Haase, M. Hennrich, F. Dubin, and J. Eschner, Heralded single-photon absorption by a single atom, Nat. Phys. **7**, 17 (2011).
[35] W. Yao, R.-B. Liu, and L. J. Sham, Theory of Control of the Spin-Photon Interface for Quantum Networks, Phys. Rev. Lett. **95**, 030504 (2005).
[36] X. Ding, Y. He, Z.-C. Duan, N. Gregersen, M.-C. Chen, S. Unsleber, S. Maier, C. Schneider, M. Kamp, S. Höfling, C.-Y. Lu, and J.-W. Pan, On-Demand Single Photons with High Extraction Efficiency and Near-Unity Indistinguishability from a Resonantly Driven Quantum Dot in a Micropillar, Phys. Rev. Lett. **116**, 020401 (2016).
[37] K. A. Fischer, R. Trivedi, V. Ramasesh, I. Siddiqi, and J. Vučković, Scattering into one-dimensional waveguides from a coherently-driven quantum-optical system, Quantum **2**, 69 (2018).
[38] M. Pechal, L. Huthmacher, C. Eichler, S. Zeytinoğlu, A. A. Abdumalikov, S. Berger, A. Wallraff, and S. Filipp, Microwave-Controlled Generation of Shaped Single Photons in Circuit Quantum Electrodynamics, Phys. Rev. X **4**, 041010 (2014).
[39] V. Averchenko, D. Sych, C. Marquardt, and G. Leuchs, Efficient generation of temporally shaped photons using nonlocal spectral filtering, Phys. Rev. A **101**, 013808 (2020).
[40] V. Averchenko, D. Sych, G. Schunk, U. Vogl, C. Marquardt, and G. Leuchs, Temporal shaping of single photons enabled by entanglement, Phys. Rev. A **96**, 043822 (2017).
[41] P. Forn-Díaz, C. W. Warren, C. W. S. Chang, A. M. Vadiraj, and C. M. Wilson, On-Demand Microwave Generator of Shaped Single Photons, Phys. Rev. Appl. **8**, 054015 (2017).
[42] G. S. Vasilev, D. Ljunggren, and A. Kuhn, Single photons made-to-measure, New J. Phys. **12**, 063024 (2010).
[43] P. B. R. Nisbet-Jones, J. Dilley, D. Ljunggren, and A. Kuhn, Highly efficient source for indistinguishable single photons of controlled shape, New J. Phys. **13**, 103036 (2011).
[44] J.-R. Álvarez, M. IJspeert, O. Barter, B. Yuen, T. D. Barrett, D. Stuart, J. Dilley, A. Holleczek, and A. Kuhn, How to administer an antidote to Schrödinger's cat, J. Phys. B: At., Mol. Opt. Phys. **55**, 054001 (2022).
[45] E. Rephaeli and S. Fan, Stimulated Emission from a Single Excited Atom in a Waveguide, Phys. Rev. Lett. **108**, 143602 (2012).
[46] K. R. Brown, K. M. Dani, D. M. Stamper-Kurn, and K. B. Whaley, Deterministic optical Fock-state generation, Phys. Rev. A **67**, 043818 (2003).
[47] H. Eleuch, S. Guérin, and H. R. Jauslin, Effects of an environment on a cavity-quantum-electrodynamics system controlled by bichromatic adiabatic passage, Phys. Rev. A **85**, 013830 (2012).
[48] M. Amniat-Talab, S. Lagrange, S. Guérin, and H. R. Jauslin, Generation of multiphoton Fock states by bichromatic adiabatic passage: Topological analysis, Phys. Rev. A **70**, 013807 (2004).
[49] A. Gogyan, S. Guérin, C. Leroy, and Y. Malakyan, Deterministic production of *n*-photon states from a single atom-cavity system, Phys. Rev. A **86**, 063801 (2012).
[50] A. Gogyan, S. Guérin, H.-R. Jauslin, and Y. Malakyan, Deterministic source of a train of indistinguishable single-photon pulses with a single-atom-cavity system, Phys. Rev. A **82**, 023821 (2010).
[51] C. W. Gardiner and P. Zoller, *Quantum Noise*, 3rd ed. (Springer, New York, 2004).
[52] R. Loudon, *The Quantum Theory of Light* (Clarendon, Oxford, 2000).
[53] H. P. Breuer and F. Petruccione, *The Theory of Open Quantum Systems* (Oxford University Press, Oxford, 2002).
[54] C. Tserkezis, A. I. Fernández-Domínguez, P. A. D. Gonçalves, F. Todisco, J. D. Cox, K. Busch, N. Stenger, S. I. Bozhevolnyi, N. A. Mortensen, and C. Wolff, On the applicability of quantum-optical concepts in strong-coupling nanophotonics, Rep. Prog. Phys. **83**, 082401 (2020).
[55] V. Dorier, S. Guérin, and H.-R. Jauslin, Critical review of quantum plasmonic models for finite-size media, Nanophotonics **9**, 3899 (2020).
[56] B. Rousseaux, D. Dzsotjan, G. Colas des Francs, H. R. Jauslin, C. Couteau, and S. Guérin, Adiabatic passage mediated by plasmons: A route towards a decoherence-free quantum plasmonic platform, Phys. Rev. B **93**, 045422 (2016).
[57] S. M. Dutra, *Cavity Quantum Electrodynamics: The Strange Theory of Light in a Box* (Wiley, Hoboken, NJ, 2005).
[58] M. Scala, B. Militello, A. Messina, J. Piilo, and S. Maniscalco, Microscopic derivation of the Jaynes-Cummings model with cavity losses, Phys. Rev. A **75**, 013811 (2007).
[59] M. Scala, B. Militello, A. Messina, S. Maniscalco, J. Piilo, and K.-A. Suominen, Cavity losses for the dissipative Jaynes–Cummings Hamiltonian beyond rotating wave approximation, J. Phys. A: Math. Theor. **40**, 14527 (2007).
[60] G. L. Giorgi, A. Saharyan, S. Guérin, D. Sugny, and B. Bellomo, Microscopic and phenomenological models of driven systems in structured reservoirs, Phys. Rev. A **101**, 012122 (2020).
[61] W. Vogel and D.-G. Welsch, *Quantum Optics*, 3rd ed. (Wiley-VCH, New York, 2006).
[62] K. J. Blow, R. Loudon, S. J. D. Phoenix, and T. J. Shepherd, Continuum fields in quantum optics, Phys. Rev. A **42**, 4102 (1990).
[63] C. K. Law and H. J. Kimble, Deterministic generation of a bit-stream of single-photon pulses, J. Mod. Opt. **44**, 2067 (1997).
[64] K. M. Gheri, K. Ellinger, T. Pellizzari, and P. Zoller, Photon-wavepackets as flying quantum bits, Fortschr. Phys. **46**, 401 (1998).
[65] L. Knöll, W. Vogel, and D.-G. Welsch, Resonators in quantum optics: A first-principles approach, Phys. Rev. A **43**, 543 (1991).

[66] I. S. Murray, M. O. Scully, and W. E. Lamb, Jr., *Laser Physics* (Avalon, New York, 1978).

[67] B. J. Dalton, S. M. Barnett, and B. M. Garraway, Theory of pseudomodes in quantum optical processes, Phys. Rev. A **64**, 053813 (2001).

[68] In the simulation we use the actual response function ($B1$) derived for a single-layer mirror with a thickness $\delta = \lambda_c/(4n)$, and the atom is placed at $x_a = -L/2$.

[69] R. Graham and H. Haken, Quantum theory of light propagation in a fluctuating laser-active medium, Z. Phys. A: Hadrons Nuclei **213**, 420 (1968).

[70] M. G. Raymer and C. J. McKinstrie, Quantum input-output theory for optical cavities with arbitrary coupling strength: Application to two-photon wave-packet shaping, Phys. Rev. A **88**, 043819 (2013).

[71] W. H. Louisell, *Quantum Statistical Properties of Radiation* (Wiley, New York, 1973).

[72] H. J. Carmichael, *Statistical Methods in Quantum Optics* (Springer, Berlin, 1999).

[73] A. Kuhn, M. Hennrich, T. Bondo, and G. Rempe, Controlled generation of single photons from a strongly coupled atom-cavity system, Appl. Phys. B **69**, 373 (1999).

[74] M. Keller, B. Lange, K. Hayasaka, W. Lange, and H. Walther, A calcium ion in a cavity as a controlled single-photon source, New J. Phys. **6**, 95 (2004).

[75] B. W. Shore, *Manipulating Quantum Structures Using Laser Pulses* (Cambridge University Press, Cambridge, 2011).

[76] D. V. Reddy and M. G. Raymer, Photonic temporal-mode multiplexing by quantum frequency conversion in a dichroic-finesse cavity, Opt. Express **26**, 28091 (2018).

[77] S. Krastanov, K. Jacobs, G. Gilbert, D. R. Englund, and M. Heuck, Controlled-phase gate by dynamic coupling of photons to a two-level emitter, npj Quantum Inf. **8**, 103 (2022).

[78] J. I. Cirac, L. M. Duan, and P. Zoller, Quantum optical implementation of quantum information processing, in *Experimental Quantum Computation and Information*, Vol. 148, edited by F. De Martini and C. Monroe (IOS Press, Amsterdam, 2002), p. 263.

[79] D. Griffiths and S. Walborn, Dirac deltas and discontinuous functions, Am. J. Phys. **67**, 446 (1999).

[80] A. Saichev and W. Woyczynski, *Distributions in the Physical and Engineering Sciences, Volume 1: Distributional and Fractal Calculus, Integral Transforms and Wavelets* (Birkhäuser, Boston, 1997).